Penultimate interglacial palynology of Flanders

Van Beirendonck, Filip; Van der Putten, Nathalie; Verbruggen, Cyriel

published in
Quaternary Science Reviews
2023

DOI (link to publisher)
10.1016/j.quascirev.2023.108113

document version
Publisher's PDF, also known as Version of record

Quaternary Science Reviews 310 (2023) 108113

Contents lists available at ScienceDirect

Quaternary Science Reviews

journal homepage: www.elsevier.com/locate/quascirev

Penultimate interglacial palynology of Flanders: A revised river evolution model

Filip Van Beirendonck [a, *], Nathalie Van der Putten [b], Cyriel Verbruggen [a]

[a] Department of Geology, Faculty of Sciences, Ghent University, Krijgslaan 281, BE-9000, Gent, Belgium
[b] Department of Earth Sciences, Faculty of Sciences, VU Amsterdam, De Boelelaan 1105, NL-1081, Amsterdam, the Netherlands

ARTICLE INFO

Article history:
Received 3 March 2023
Received in revised form
27 April 2023
Accepted 30 April 2023
Available online 16 May 2023

Handling Editor: Donatella Magri

Keywords:
late Middle Pleistocene
Paleoclimatology
Northwest Europe
Palynology

ABSTRACT

There are no Saalian Stage pollen records in Northwest Europe that not only cover an entire interglacial complex but also have been successfully correlated down to marine isotope substage level. The presented pollen record fills this knowledge gap. Three pollen sequences, sampled from a well-preserved Saalian Stage river terrace near Brussels (Belgium), together span most of an interglacial complex: two interglacial cycles and one interstadial separated by colder intervals. To date the pollen data, the authors present a multi-proxy supported river evolution model through which the correlation of the pollen record with the penultimate interglacial complex (Marine Isotope Stage (MIS) 7) becomes apparent. The authors further illustrate homotaxis—defined as the similarity between pollen diagrams that are not necessarily contemporaneous—by comparing MIS 7 with MIS 5 pollen data from the same area, convincingly curve-match the pollen record with marine isotope data, and point to similarities between Southern and Northwest European vegetation dynamics and climate variability during MIS 7.

1. Introduction

Compared to the palynological record of the Eemian (Cleveringa et al., 2000; Felde et al., 2020; Turner, 2000; Zagwijn, 1961, 1996) and Holsteinian (Benda et al., 1993; Diehl and Sirocko, 2007; Hallik, 1960), that of the intermediate Saalian Stage in Northwest Europe (Cohen and Gibbard, 2019; Litt and Turner, 1993) is not well known. Classics from northern Germany are Wacken (Menke, 1968), Pritzwalk and Kap Arkona (Dömnitz and Rügen Warmzeit, Erd, 1970; 1973), and Röpersdorf (Uecker Warmzeit, Erd, 1987). In Denmark (Vejlby I/II, Andersen, 1965) and the Netherlands (Hoogeveen/Bantega, Zagwijn, 1973), palynologists recorded two related warm phases separated by a short cold interval. Despite previous attempts (*e.g.*, de Beaulieu et al., 2001), however, none of these pollen sequences have so far been satisfactorily placed in a palynostratigraphic framework, as they rarely span a complete interglacial cycle (Birks and Birks, 2004; pollen analysts' definition, Suggate, 1965). The age determination of longer and/or better studied Saalian Stage pollen records, on the other hand, seems to rely heavily on experimental age estimates from geochronological methods (Kleinmann et al., 2011; Preusser et al., 2005; Schokker et al., 2005; Tucci et al., 2021; Urban, 1995, 2007; Urban et al., 1991) and/or to be directed by the preferred landscape evolution model (Wansa, 2019). Ideally, these pollen sequences should be compared with well-dated Northwest European type sections spanning one or more Saalian Stage interglacial complexes (odd-numbered marine isotope stages, Railsback et al., 2015; Schirmer, 2010), like in Southern Europe—for convenience, including the French Massif Central—(Desprat et al., 2006; Follieri et al., 1988; Koutsodendris et al., 2023a; Okuda et al., 2001; Reille et al., 1998, 2000; Roucoux et al., 2006, 2008; Sadori et al., 2016). There are currently, however, no Saalian Stage pollen records in Northwest Europe that not only cover an entire interglacial complex but also have been successfully correlated down to marine isotope substage level.

The following pollen record fills this knowledge gap. We present three pollen diagrams from well-preserved Saalian Stage floodplain deposits. We aim to demonstrate that the vegetation dynamics recorded in this pollen record reflects the climate variability during the marine isotope substages of the penultimate interglacial complex (MIS 7). To realize this goal, we first introduce a multi-proxy supported river evolution model that allows to make a distinction between different river styles during MIS 7 (meandering), 6

* Corresponding author.
E-mail addresses: filip.vanbeirendonck@ugent.be (F. Van Beirendonck), n.n.l.vanderputten@vu.nl (N. Van der Putten), cyriel.verbruggen@ugent.be (C. Verbruggen).

https://doi.org/10.1016/j.quascirev.2023.108113
0277-3791/

(braided), and 5 (meandering), and to connect the pollen record with MIS 7 river activity in the study area. To exclude other possibilities, we confront the pollen record from MIS 7 floodplain deposits with an Eemian-Weichselian Early Glacial (MIS 5) pollen composite from the same area. We discuss the reliability of our conclusions by curve-matching the pollen record with marine isotope and Southern European pollen sequences, and by demonstrating similarities in vegetation dynamics and climate variability during MIS 7 across Europe.

2. Regional setting (Fig. 1A and B)

The study area extends north of Brussels and southwest of Mechelen along the left bank of the lower Senne (Fig. 1A). In its upper reaches, the river cuts through Palaeozoic rocks of the Brabant Massif (Herbosch and Debacker, 2018), of which Fig. 1A shows the northern outcrop zone (BMN). Past Halle, Paleogene (mainly Eocene) glauconitic sands and clays dominate the pre-Quaternary geology of the Senne basin (Buffel and Matthijs, 2009; Buffel et al., 2009). Southwest of the study area, younger Neogene sediments cap the hilltops (NEO, Louwye et al., 2020). Their basal deposits consist of an extensive flint pebble bed. At some places, the Neogene sediments thin out so that only loess covers this gravel bed (Leriche, 1934-1935). Southwards along the left bank of the Senne, loess accumulations more than 20 m thick are not exceptional (*e.g.*, Halet and Lejeune de Schiervel, 1905). Northwards from these Neogene hilltops, however, the topography becomes much more subdued and the aeolian cover thinner and sandier. This vast region is called the 'Belgian sand belt' (Beerten et al., 2017). In this wide rural plain north of Vilvoorde, elevation gradually decreases from 20 to 10 m TAW (Belgian Ordnance Datum) and still lower in the Senne floodplain (Fig. 1B). The Brussels-Scheldt Maritime (B–S M) Canal cuts through the study area, which today is drained by only small brooks and man-made ditches.

Quaternary geological research in the study area started at the end of the 19th century (Rutot and Van den Broeck, 1892): particularly between Vilvoorde and Kapelle-op-den-Bos (Fig. 1A), workers described peaty units called 'Tourbes quaternaires anciennes' (*e.g.*, B5 & B6, Fig. 1B). Further research, however, had to wait until the construction of the Zemst Sea Lock (ZSL, Gulinck et al.,

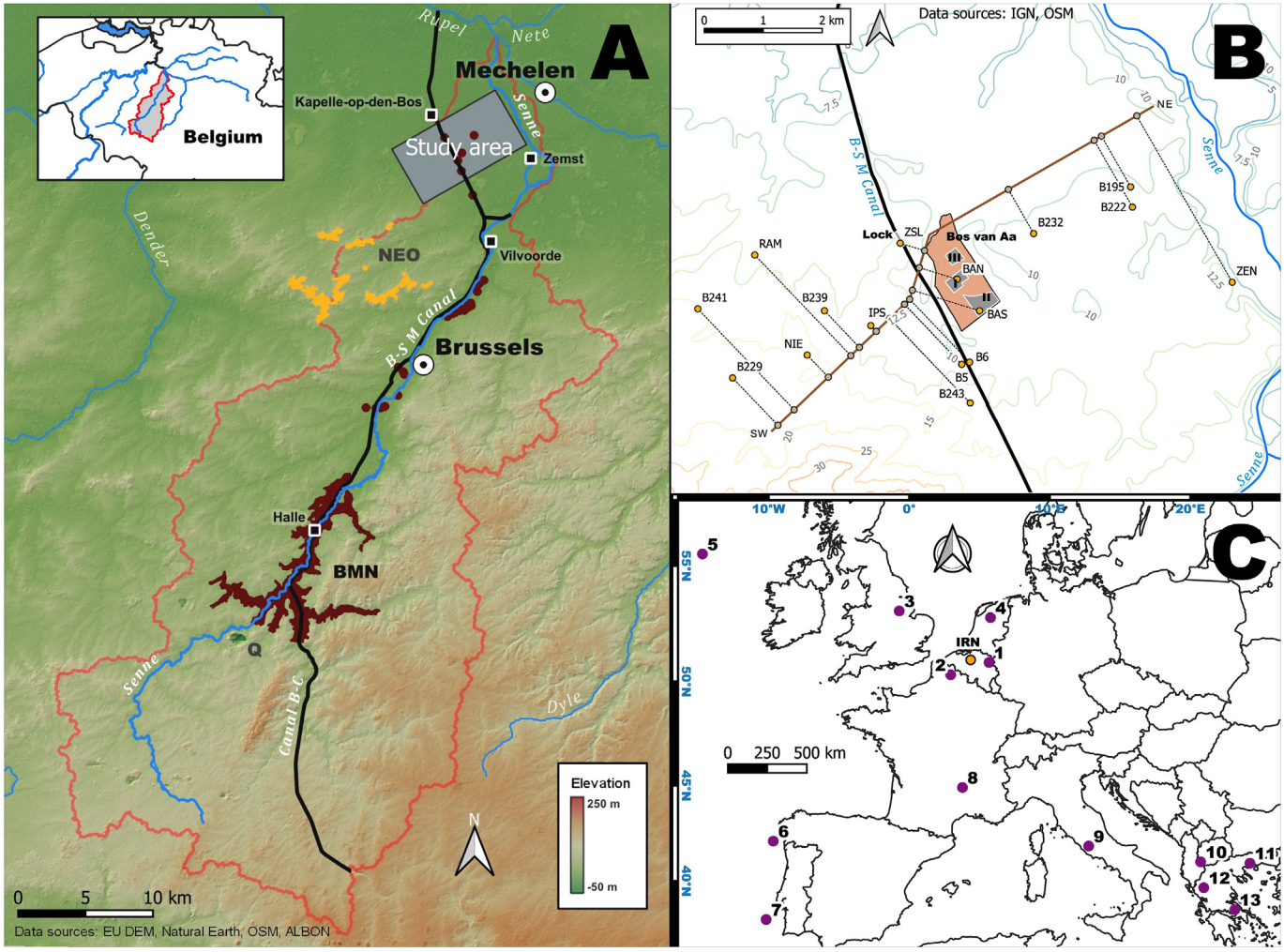

Fig. 1. A. Regional setting, Inset: Scheldt river basin, Scheldt = thickest line; Main: Senne river basin with Study area; BMN = Brabant Massif Northern outcrop zone, NEO = Neogene hilltops, Q = Quenast quarry depression, B–S M = Brussels-Scheldt Maritime Canal, B–C = Canal Brussels-Charleroi; Palaeozoic clasts in subsurface (brown •, App. E) indicate a former course of the Senne
B. Study area with locations of boreholes and excavation sites (Bos van Aa pits I-III and Lock pit: BAN, BAS, and ZSL are synthesis profiles handled as point data in Fig. 2); projection line (SW-NE, Fig. 2); contour lines in m TAW (Belgian Ordnance Datum), interval contour lines >15 m TAW = 5 m, <15 m TAW = 2.5 m; B–S M = Brussels-Scheldt Maritime Canal
C. European sites mentioned in text: Maastricht-Belvédère (1), Biache-Saint-Vaast (2), Balderton terrace (3), Bantega (4), Ocean Drilling Program (ODP) site 980 (5), MD01-2447 (6), MD01-2443 (7), Lac du Bouchet (8), Valle di Castiglione (9), Lake Ohrid (10), Tenaghi Philippon (11), Ioannina (12) & Lake Kopais (13).

1971). Not much later, the Geological Survey of Belgium launched a drilling campaign to study the lithology of the Quaternary deposits (Bogemans, 1988; Bogemans and Paepe, 1982). Several cores proved fruitful for palynological analysis (Verbruggen, 1999 and this study). Bogemans (1983, 1988) also described profiles from sand extraction pits in Bos van Aa (Fig. 1B), which are renowned for their rich collection of mammalian remains (Germonpré, 1985, 1986, 1993, 2003) and archaeology (Bogemans and Caspar, 1984; Van Peer and Smith, 1990). Bos van Aa has now become a nature reserve after backfilling of the pits. Bogemans (1988, 1993) synthesized all observations in a (chrono)stratigraphic framework that is still largely in use today (Germonpré et al., 1993; Heyse and Demoulin, 2018). Essential in this facies model is the vertical succession of two distinct river styles: meandering and braided (Bogemans, 1993, 1996). We supplement the results of all the above-mentioned studies with hitherto unpublished pollen data, and revise the facies model and (chrono)stratigraphy.

3. Material and methods

The sediment cores (IPSvoorde, RAMsdonk & NIEuwenrode) were brought to the surface using a mechanized drilling unit with the possibility of retrieving undisturbed 1 m-long cores. The 10-cm wide cores were split into halves. One half was used to describe lithology (App. A), and the other was sampled for palynological analysis.

The three pollen sequences (IPS, RAM & NIE) mainly consist of an alternation of organic mud and peat beds. IPS (Fig. 3), from 6.54 to 10.72 m below surface (mbs), mainly consists of an alternation of organic mud/clay and peat beds with a sterile sand layer at 8–8.62 mbs. The whole sequence is truncated by a coarse gravel layer (6.1–6.5 mbs). RAM (Fig. 4, 3.38–5.4 mbs) is mainly composed of organic mud merging upwards into a peat bed (3.38–3.58 mbs). The latter is truncated by a coarse gravel layer (3–3.38 mbs). NIE (Fig. 3, 5.11-6.33 mbs) consists of 1 m organic mud merging upwards into a c. 20 cm thick peat bed (5.11–5.34 mbs).

The laboratory technique of all pollen sequences was carried out by C. Verbruggen in the 1970s and '80s. The samples, obtained at 2–5 cm intervals, were treated following the classical methodology of Fægri & Iversen (Fægri et al., 1964), modified by using Thoulet's solution for gravitation-separation (*e.g.*, Goeury and Beaulieu, 1979). The microfossils were mounted in glycerine-gelatine and counted with a light microscope at a magnification of 400 and 1000 × (oil immersion) and the pollen types were identified using a personal reference collection, Erdtman et al. (1961), Fægri et al. (1964), and Moore and Webb (1978) or, in case of doubt, by contacting the Palynology Lab of Utrecht University. From Ipsvoorde, 148 levels were analysed (pollen sum M = 391, SD = 137.23), 56 from Ramsdonk (M = 366, SD = 62.04), and 40 from Nieuwenrode (M = 249, SD = 99.43). In general, pollen preservation was good (but see section 4.2.3).

The pollen spectra were visualized as percentage pollen diagrams relative to the pollen sum (Figs. 3, 4 and 7). The pollen sum includes total arboreal pollen (AP = trees and shrubs, curves in colour) and non-arboreal pollen (NAP = herbs including Ericaceae, in black), excluding non-pollen palynomorphs (spores and algae) and pollen of aquatics (all in grey). TILIA software (version 3.0.1.; ©1991–2020 Eric C. Grimm) was used to carry out percent calculation and cluster analysis (CONISS, sum of square roots, Grimm, 1987), and to visualize the pollen diagrams. The pollen data were divided into Pollen Assemblage Zones (PAZ) based on the results of the CONISS algorithm and personal judgment. All pollen diagrams share the same y-axis that expresses elevation in m TAW. We refer to App. B for the raw pollen data.

Two datasets were used to construct the geological cross-section in Fig. 2. The first are borehole data that were retrieved from the Database Subsurface Flanders (DOV). Most (except B5 & B6) are cored borings from surveys in the 1970s and '80s. The second dataset are profile drawings and descriptions from Bos van Aa pits I & II and the Lock pit (Bogemans, 1988; Gulinck et al., 1971). These were synthesized into condensed profiles (BAS, BAN & ZSL) and handled as point data (Fig. 1B). In fact, two synthesis profiles were constructed for pit II because, as extraction works proceeded southwest, sedimentology and stratigraphy considerably changed between the observation years 1983 (**R**) and 1986 (**L**) (BAS, Fig. 2, Bogemans, 1988). We refer to App. C1 for borehole data and additional information. Observations or proxies were only added to Fig. 2 provided their exact position—essentially elevation—was explicitly mentioned in one of the following references (App. C2): Bogemans (1983, 1988, 1993), Bogemans and Caspar (1984) and Gulinck et al. (1971).

4. Results and interpretation

4.1. Cross-section: sedimentary units (Fig. 2, App. C2)

Unit 0 figures the Paleogene substratum, not reached in some boreholes (B239, IPS, BAN & B222, **?**, Fig. 2).

Unit 1 is a coarse green sand to gravel (NIE). Grain size and colour suppose reworking of the Paleogene (high glauconite content).

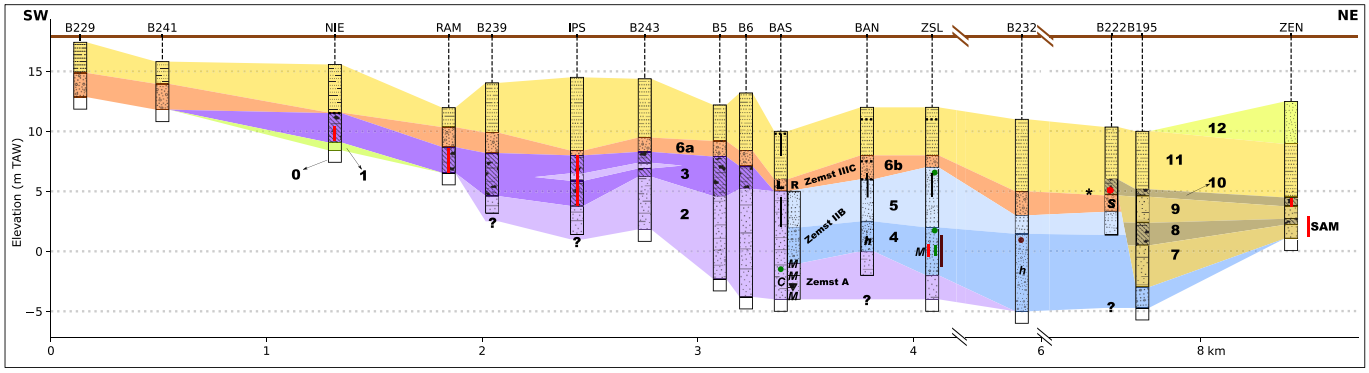

Fig. 2. Cross-section along projection line (SW-NE, Fig. 1B), vertical exaggeration x 55, distance left and right from B232 shortened for readability; Paleogene substratum (0), **?** depth unknown; Quaternary Sedimentary Units (1–12, see text), * insufficient data to exclude the possibility of a post-Unit 10 incision; Symbology observations or proxies: palynology in red (bars and circles), location SAM see No. 13, Fig. 6; macro-remains in green; Palaeozoic clasts in brown; ***C*** *Corbicula fluminalis*; ***M*** Mammal remains; ▼ archaeology; ***h*** clay nodules or lenses, reworked peat and wood fragments; ▪▪▪ gravel lags; **|** pseudomorphs of epigenetic cryogenic fissures; ***S*** Soil complex; **L R** split synthesis profiles to reflect changing sedimentology and stratigraphy over time (1986 versus 1983, BAS); fossil mammal assemblages Zemst A-IIB-IIIC from Bos van Aa pits I & II (Germonpré, 2003).

Unit 2 is mainly sand-sized. Finer-grained silt to clay layers, often organic or with washed in plant remains, alternate with this generally silty or clayey sand (observations in Bos van Aa pits I & II, Fig. 1B). The primary sedimentary structures signify natural levee and point bar deposits (Bogemans, 1983, 1988, 1996). Similar channel deposits at the base of pit II (BAS) are often sandier and may contain gravel (flint and sandstone), intact bivalves (*Corbicula fluminalis*, ***C***), plant macro-remains suggestive of temperate climatic conditions (green •), and *in situ* artefacts (▼) (Bogemans and Caspar, 1984) and mammalian bones (***M***) (assemblage Zemst A, Germonpré, 2003, App. C5). The nature, distribution, and concentration of these fossils and lithics assume deposition on a point bar of a meandering river channel close to a wooded area in a temperate climate (Buckingham *in* Scott and Buckingham, 2021).

Unit 3 mainly consists of organic mud and peat, which accumulated on the floodplain of a single thread river (IPS, RAM & NIE, red bars). Closer to the former meandering channel belt, the sediment coarsens and sporadic sand layers appear. The sandy intercalation (IPS)—crevasse splay (see Section 4.2.1)?—is classified as Unit 2.

Units 2–3 represent two facies of the same single thread meandering river system (Bogemans, 1988, 1993): sandy channel and bank deposits on the one hand (Unit 2: BAS, BAN & ZSL), and fine-grained organic floodplain deposits on the other (Unit 3: IPS, RAM & NIE).

Unit 4 is a mostly gravel-rich coarse sand—with remains of mammoth and woolly rhinoceros (ZSL, ***M***)—but with considerable variation in granulometry, in places only gravel, sometimes siltier, with clay nodules or lenses, reworked peat and wood fragments (BAN & B232, ***h***). The presence of plant remains typical for a temperate alluvial wetland (green bar and •, App. C3) and interglacial pollen spectra from a peat lump (red bar) (ZSL, Vanhoorne *in* Gulinck et al., 1971) suggest that redeposition of meandering river deposits (Units 2–3) took place in a high-energy fluvial environment. The severity and nature of this rejuvenation event is best demonstrated by the local presence of Palaeozoic clasts of the Brabant Massif (ZSL & B232, brown bar and •), also more upstream along the river Senne (Van der Sluys, 1996, App. E). These rocks outcrop to the north of Halle (BMN, Fig. 1A); the distribution of Palaeozoic clasts north of this outcrop zone (brown •, Fig. 1A) proves severe regressive erosion of the hinterland during deposition of Unit 4.

Unit 5 represents a fine to medium sand with silt inclusions and channel gravel lags (BAS, BAN & ZSL). The primary sedimentary structures are typical for a sandy braided river (Bogemans, 1988, 1993; Gulinck et al., 1971), with evidence for a standstill towards its top (see Unit 6 for a further discussion).

Units 4–5 are the result of fluvial activity and deposition by a multi thread braided river system. Overall, competence decreases towards the top, but signs of renewed erosion at the base of Unit 5 clearly divides this sediment stack in two Units (Bogemans, 1988, 1993; Gulinck et al., 1971).

Unit 6 is divided into two localized subunits: in the first area, Unit 6 truncates Unit 3 or covers the Paleogene substratum (Unit 6a), but it constitutes the top of Unit 5 in the second (Unit 6b). In each area, a different depositional process dominated.

Unit 6a (IPS, RAM & NIE) is a mixture of silt or clay layers with gravel (flint and sandstone, sometimes pebble-sized) in a mostly coarse sandy matrix (Bogemans, 1988, 1993, 1996), at places reduced to only a flint gravel string (NIE, ▪▪▪) or a flint pebble lag (IPS). In the vicinity of NIE (Fig. 1B), Unit 6a orients transverse to the main river system and grain size decreases to the east (Bogemans, 1993). The absence of Palaeozoic clasts (see Unit 4) and its large size, plead for a local origin of the gravel (NEO, Fig. 1A). Unit 6a is a lag deposit resulting from slope processes under periglacial conditions and the subsequent removal of fines by run-off and deflation.

Unit 6b was observed in Bos van Aa (Bogemans, 1988) and the Lock pit (Gulinck et al., 1971). Bogemans (1988) described a rust-coloured gravel-rich coarse sand (BAN), sometimes sandier with only channel gravel lags and discontinuous clay layers. Signs of deflation (BAN, ▪▪▪) and deep frost penetration (BAS, BAN, ZSL, |) suggest a cold and dry climate towards the end of Unit 5 and during Unit 6b. Wetter conditions, however, might have preceded this cold and dry phase given the presence of abundant macro-remains of a tundra plant (green •) (ZSL, Vanhoorne *in* Gulinck et al., 1971, App. C4) and an intact mandible of the collared lemming (*Dicrostonyx torquatus*) (assemblage Zemst IIIC, Germonpré, 2003), which is now widely distributed in the Arctic tundra (Sutcliffe and Kowalski, 1976).

Relict features in these exposures (Unit 6b) suggest the remains of a paleosol. Besides the already mentioned rusty colour (BAN), Paepe (*in* Gulinck et al., 1971) described Unit 6 (ZSL) as reddish gravel with rubified sand, oxidation zones, and Fe–Mg concretions. Similar features were described from sediment cores (Unit 6a, App. C1). Rubification or pedogenic hematite formation (Kemp, 1985) is taken as evidence of temperate weathering during interglacials (Brandon and Sumbler, 1991), and therefore indicate warmer conditions after formation of a lag deposit. More to the northeast and in a lower position (B222), Bogemans (1988) reported an organic-rich soil complex in a medium gravelly sand that resembles a gleysol (***S***).

Unit 6 is an important marker horizon suggestive of a standstill, first with erosion (lag deposit), then formation of an interglacial soil.

Units 7–10 occur near the current alluvial plain of the river Senne (Fig. 1B). Primary sedimentary structures demonstrate two facies of a meandering river system (Bogemans, 1988, 1993). Units 7 and 9 are the mostly fine to medium sandy channel and bank deposits, with a mixture of silt and clay, whereas Units 8 and 10 mainly consist of peat. Verbruggen (1999) analysed pollen samples from this peat that prove favourable conditions for temperate trees to grow, alternating with cold spells (SAM & ZEN, red bars).

Unit 11 covers the area with about 5 m of aeolian sand and silt (Beerten et al., 2017). The bottom 2 m in Bos van Aa and Lock pits, however, show signs of fluvial activity and contain more gravel (BAN & ZSL, Bogemans, 1988; Gulinck et al., 1971; Paepe, 1972). According to Bogemans (1983), the local fluvial system has rotated through a large angle—coming from higher terrain to the west-southwest—but its activity must have been dispersed and shallow. In the northeast, a medium to coarse sand with gravel covers Unit 10 (B222, B195 & ZEN). The gravel composition (flint, sandstone, and Nummulites) suggests renewed erosion of the Paleogene. There is, however, no indication that this erosional phase was profound, though observations in this area are scarce (left to B222, *). Signs of deep frost penetration at the top of Unit 10 (ZEN) and in the Lock pit (ZSL, Gulinck et al., 1971; Paepe, 1972) prove cold climatic conditions during or after this erosional phase. Periglacial features also appear in the uppermost 3 m of a purer aeolian facies (ZSL, Paepe, 1972), in which organic remains are scarce or altogether absent. Close to the surface, a widespread gravel string and associated cryogenic fissures stand out (BAS, BAN & ZSL, ▪▪▪ and |).

Unit 12 is a pure windblown sand (ZEN) that forms a low and wide ridge at the edge of the alluvial plain of the present river Senne (Fig. 1B).

A temperate-climate (podzolic) soil has developed in the top deposits (Units 11–12)..

4.2. Palynology: pollen assemblage zones (PAZ, Figs. 3 and 4)

We refer to App. D for an extended description of the Pollen

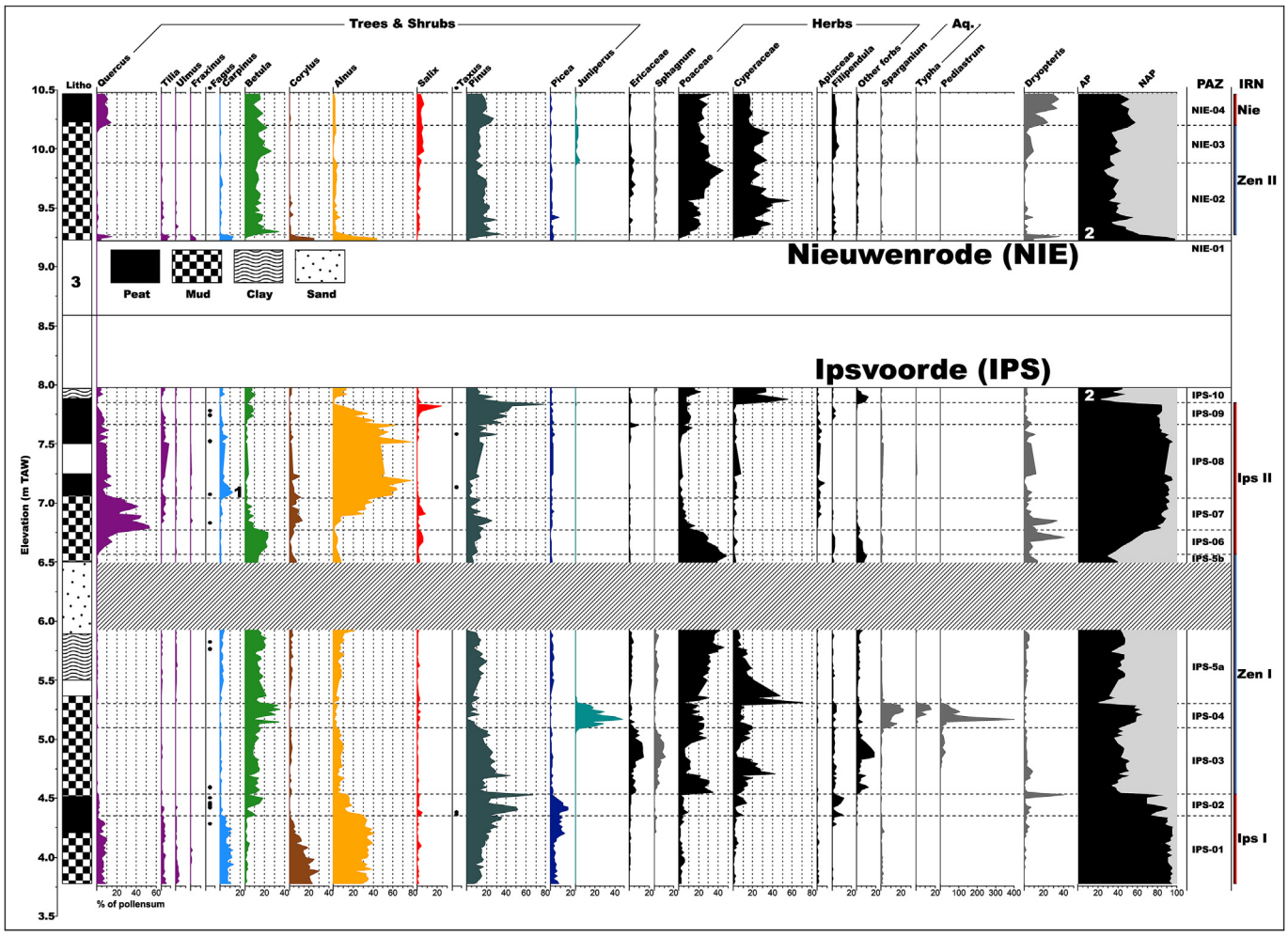

Fig. 3. Ipsvoorde (IPS) & Nieuwenrode (NIE) percentage pollen diagrams (location see Figs. 1B and 2) of selected taxa (Other forbs = sum forbs except Apiaceae and *Filipendula*, Aq. = Aquatics), spacing gridlines 10%, hatched = sterile, white space Litho column between 7.5–7.25 and 5.5–5.37 m TAW = core loss, individual curves in colour = AP (• presence *Fagus* and *Taxus* pollen), in black = NAP, in grey = excluded from pollen sum; IPS & NIE combine to IRN sequence (right column, Fig. 8 (A)), which consists of two interglacial cycles (Ips I & II, red) and one interstadial (Nie, red) separated by colder intervals (Zen I & II, blue); nos. 1, 2 & 3 aid the reader in the correlation process (see Fig. 5): No. 1 at rise *Carpinus* curve (IPS-08) corresponds with No. 1 at rise *Carpinus* curve (RAM-04, Fig. 4), No. 2 (see AP-NAP curve) indicates where IPS & NIE overlap, No. 3 (see Litho column) indicates the gap between top RAM at 8.59 m TAW (Fig. 4) and base NIE.

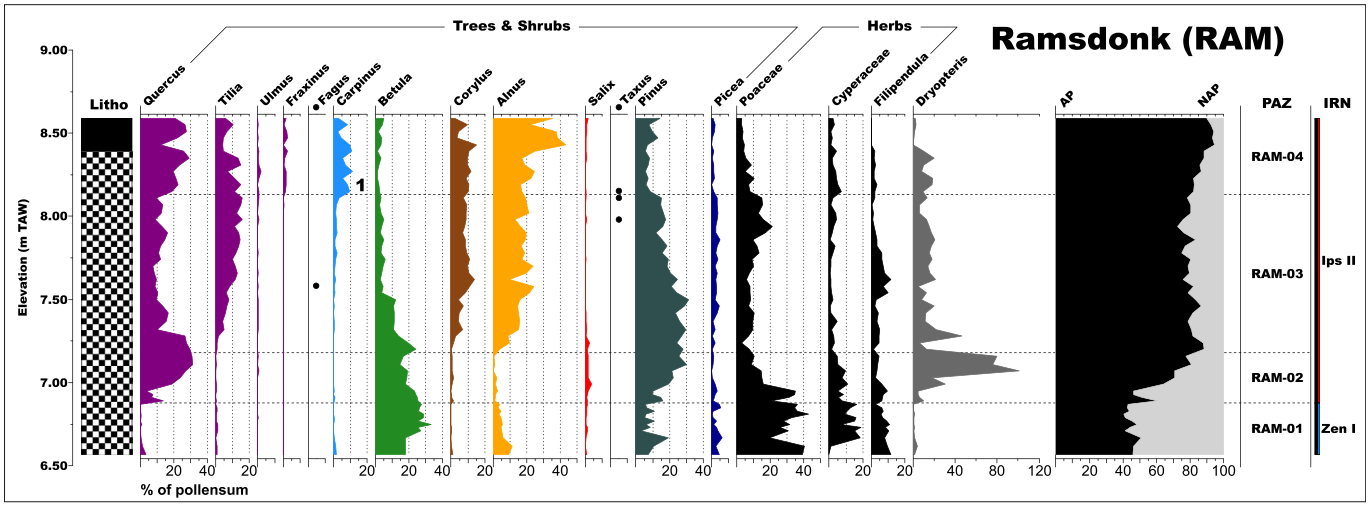

Fig. 4. Ramsdonk (RAM) percentage pollen diagram (location see Figs. 1B and 2) of selected taxa, spacing gridlines 10%, lithology see Fig. 3, individual curves in colour = AP (• presence *Fagus* and *Taxus* pollen), in black = NAP, in grey = excluded from pollen sum; No. 1 aids the reader in the correlation process (see Fig. 5): No. 1 at rise *Carpinus* curve (RAM-04) corresponds with No. 1 at rise *Carpinus* curve (IPS-08, Fig. 3), see also IRN (right column).

Assemblage Zones. The shorter version below stresses vegetation dynamics (see also Table 1).

4.2.1. Ipsvoorde (IPS, Figs. 2 and 3)

First interglacial cycle (IPS-01 & IPS-02). The vegetation at the start of *IPS-01* resembles an oak-hornbeam community (*cf. Carpinion betuli* alliance, Decleer, 2007), which rapidly retrogrades into a hemiboreal forest (pine and spruce gain importance). Stable and high *Alnus* values prove an alder carr. The presence of hornbeam, a progressive decline of hazel, and the expansion of spruce, typify the late-temperate or oligocratic zone of an interglacial cycle (zonation scheme *cf.* Turner and West, 1968). At the start of *IPS-02*, the hemiboreal forest further retrogrades into a pine and spruce dominated taiga, above which *Picea* values drop during the next deforestation phase. Lower *Alnus* values indicate the destruction of alder carr. The dominance of boreal trees, a thinning of the forest, and the virtual extinction of temperate forest trees, characterise the post-temperate zone.

Cold interval (IPS-03 to IPS-05). The expansion of grassland at the start of *IPS-03* (Poaceae values shoot up) suggests a far-reaching deforestation outside the floodplain, and is followed by the gradual development of open treeless herbaceous communities. Scattered pine, birch, and alder trees, however, survive nearby. The floodplain resembles a boreal wetland. The climate is getting colder and wetter, which results in lower evapotranspiration rates and rising ground water levels. High *Juniperus* and *Betula* values characterise *IPS-04*. The rise and fall of both taxa seem to indicate a brief warming accompanied by rising water levels in the floodplain (expansion of reed swamp plants: *Sparganium* and *Typha*). Climate is still cold, but *Typha* spp. need a mean July temperature of at least 12–13 °C to flourish (Kolstrup, 1980). Moreover, Iversen (1954) remarked that *Typha latifolia* does not reach beyond the 14 °C July isotherm in Scandinavia. A sterile uniform sand layer splits *IPS-05* in 2 subzones (5a & 5b). This interruption in the floodplain accumulation might be caused by sediment compaction due to lowering of the ground water level (Bogemans, 1993). Indeed, sharply decreasing values of aquatics and *Pediastrum* indicate falling water levels at the start of IPS-5a. Compaction of organic mud and peat creates accommodation space, which might have triggered deposition of a crevasse splay (Makaske, 2001) and only a short break in the floodplain accumulation. The pollen record of IPS-5a demonstrates a low sward of herbaceous plants typical for a mammoth steppe (Guthrie, 1990) or steppe-tundra (Chytrý et al., 2019). In such an environment, low temperatures and lack of moisture impede the growth of trees and shrubs, though stable and high *Betula* values suggest the presence of birch trees. We ascribe the stable and low *Carpinus* and *Corylus* values on the one hand, and *Picea*, Ericaceae, and *Sphagnum* on the other, to rebedding (*sensu* Andersen, 1961). The following arguments should support this hypothesis. First, values of all above-mentioned taxa simultaneously increase as the sediment changes to clay (Fig. 3). We explain this by increased alluviation of clay particles and allochthonous pollen because of degradation of the vegetation cover and peatland in the headwaters and surrounding hills (Gibbard and Lewin, 2002). Second, above the sterile sand layer in IPS-5b, sedimentation of mud resumes and pollen of the regional (*Carpinus*) and local (Ericaceae and *Sphagnum*) vegetation disappear together. Apparently, the influx of alluvial clay and secondary pollen ceased. Infill of accommodation space by a crevasse splay might have triggered an avulsion (Makaske, 2001) leaving the Ipsvoorde site outside the direct influence of river activity.

Second interglacial cycle (IPS-06 to IPS-09). Increasing *Betula* and *Pinus* values, but especially *Quercus*, demonstrate a reforestation following a climate improvement at the end of IPS-05. We classify *IPS-06* as the pre-temperate zone of a new interglacial cycle (*cf.* Turner and West, 1968). The establishment and expansion of a mixed-oak forest (oak and linden dominate) during *IPS-07* is typical for the early-temperate or mesocratic zone, while a dense alder carr re-develops. From the start of *IPS-08*, the mixed-oak forest develops into an oak-hornbeam community (*cf. Carpinion betuli* alliance, Decleer, 2007) and a second interglacial optimum has been reached. The temperate deciduous forest, however, retrogrades into a hemiboreal one as pine gains importance. We consider IPS-08 a late-temperate or oligocratic zone, based on the arrival and continuous presence of hornbeam, a progressive decline of hazel, and increasing *Pinus* values. After that (*IPS-09*), the mixed forest retrogrades into an open pine and birch dominated taiga, and sharply decreasing *Alnus* values show the complete destruction of alder carr. A return to dominance of boreal trees, a thinning of the forest, and the virtual extinction of temperate forest trees, characterise this post-temperate zone.

Cold phase (IPS-10). The reappearance of temperate forest tree pollen during *IPS-10* suggests redeposition by slope processes (App. D), as the evolution of the AP-NAP curve demonstrates a deforestation at the end of an interglacial with sedges, but also grasses, expanding their territory.

4.2.2. Ramsdonk (RAM, Figs. 2 and 4)

Cold phase (RAM-01). The presence of temperate forest tree taxa in *RAM-01* suggest redeposition, as high values of Poaceae, *Filipendula*, and *Betula* indicate an open landscape, dominated by grassland.

Interglacial cycle (RAM-02 to RAM-04). RAM-02 shows a rapid reforestation into a semi-closed oak-pine-birch forest during the pre-temperate zone of an interglacial cycle (*cf.* Turner and West, 1968). Values of insect-pollinated *Tilia* match those of *Quercus* during *RAM-03*, which proves the widespread presence of linden—pollen quantities in the air are never high with insect pollinators. Scattered pine and spruce remain in the mixed forest. In the floodplain, alder carr supplants willow thickets. The arrival of linden and hazel marks the start of the early-temperate or mesocratic zone, when a mixed-oak forest (oak and linden dominate) develops and expands. From the start of *RAM-04*, the pollen record resembles an oak-hornbeam forest community (*cf. Carpinion betuli* alliance, Decleer, 2007) and the climate optimum has been reached. The arrival and expansion of hornbeam prove the start of a late-temperate or oligocratic zone.

4.2.3. Nieuwenrode (NIE, Figs. 2 and 3)

End of interglacial (NIE-01). NIE-01 counts only 2 pollen spectra with high values of temperate deciduous trees, showing interglacial conditions from the start. Especially AP values (99%) of the lower spectrum (pollen sum 101), however, are suspiciously high and biased towards the more robust and distinctive pollen types (Havinga, 1967). Silicification (mineralisation) processes, which C. Verbruggen noticed during fieldwork (App. A), suggest differential destruction of pollen grains. The uppermost NIE-01 spectrum (pollen sum 103), however, already shows a different vegetation pattern with the detection of graminoids and *Betula* pollen, and higher *Pinus* and *Picea* values. This expansion of boreal trees typifies the end of a temperate event, followed by a deforestation in the first spectrum of NIE-02 (pollen sum 148), in which herbaceous grassland communities expand—AP drops.

Cold interval (NIE-02 & NIE-03). An open pine-birch vegetation replaces the temperate deciduous forest, but values of both Poaceae and Cyperaceae climb above 20% from the start of *NIE-02*, indicating a far-reaching deforestation. Stable values of *Pinus*, *Betula*, and graminoids, are reminiscent of a forest steppe (Erdős et al., 2018) where sedges thrive on the floodplain, dry grassland grows on well-drained slopes and in dry plains, and an open pine-birch

forest takes in the moister slopes (Kuneš et al., 2008). According to Hoek (1997a, b), the combination of a juniper, willow, and birch expansion during *NIE-03*, together with higher values of a forb such as *Filipendula*, proves higher temperatures after a cold phase. Also, increasing *Quercus* values at the top introduce a reforestation, but dry grass- and shrubland remain dominant.

Start of interstadial (NIE-04). The return of oak and higher *Pinus* values during *NIE-04* suggests a shift from shrubland to forest, but Poaceae values remain high. According to Erdős et al. (2018), both oak and birch are common components of a forest-steppe, which we imagine to be the vegetation type in the area.

5. Discussion

5.1. Recapitulation

We demonstrated the remains of two meandering (Units 2–3 & 7–10) and one braided river system (Units 4–5) in the subsurface of the study area (Figs. 1B and 2, see Section 4.1). Multiple proxies prove predominantly temperate climatic conditions during meandering river activity, whereas a cold climate prevailed during the deposition of Units 4–5. Senne river activity gradually shifted to the east—the current river flows even more eastwardly—until finally, (fluvio-)aeolian cold climate deposits (Units 11–12) covered the area. The nature of the underlying Unit 6, first transformed into a lag deposit, then attacked by soil processes, indicates a standstill.

We also introduced three pollen diagrams (IPS, RAM & NIE, Figs. 3 and 4) and described the individual Pollen Assemblage Zones (PAZ, see Section 4.2). The longest, Ipsvoorde (IPS, Fig. 3), reveals two interglacial cycles and one intervening cold interval. The pollen record of the first interglacial cycle (IPS-01 & IPS-02) doesn't start until after the climate optimum. The botanical evolution of the next cold interval, however, is captured complete (IPS-03 to IPS-05), interrupted only by a momentary river influence (avulsion?, hatched Fig. 3), which had little or no effect on the continuity of the pollen curves. The sudden rise and fall of *Juniperus* in the middle of this cold interval (IPS-04) seem to indicate a brief warming, after which a cold steppe-like vegetation develops (IPS-05). The next interglacial cycle, which starts with the early arrival of oak (IPS-06), is also captured complete (IPS-06 to IPS-09). Oak also pioneers in the next Ramsdonk diagram (RAM, Fig. 4), which shows a decapitated interglacial cycle. The last Nieuwenrode diagram (NIE, Fig. 3) starts at the very end of an interglacial (NIE-01) before the vegetation develops into a forest steppe (NIE-02 & NIE-03) and oak returns during an interstadial (NIE-04, Turner, 1998).

5.2. Construction of the IRN pollen sequence

5.2.1. Pollen samples of a single interglacial complex (Fig. 5)

We deduce from the pollen diagrams (Figs. 3 and 4) and positions (Figs. 1B and 2)—horizontal and vertical—of IPS, RAM & NIE that the pollen sequences were sampled from an uninterrupted floodplain accumulation of a single interglacial complex (*sensu* Schirmer, 2010). We therefore expect a similar vegetational development—or pollen zone—to occur at about the same elevation. Differences, especially when they amount to several metres, call for an explanation (Fig. 5).

We correlate pollen zones RAM-02 & 03 with IPS-06 & 07 using as a marker the point where *Carpinus* values rise (No. 1, Figs. 3–5). The succession and values of the tree taxa in these pollen zones—*Quercus* and *Tilia* dominate the mixed-oak forest—indicate a similar regional vegetation, just like the synchronous early arrival of oak and pine. The latter supports the correlation of RAM-02 with IPS-06. Synchronisation is also in lithology: organic mud changes into peat where *Carpinus* culminates. We ascribe differences in relative pollen abundance to local factors, such as distance to the forest edge. The difference in elevation between the point where *Carpinus* values rise in RAM and IPS (No. 1) amounts to 1.09 m (Fig. 5).

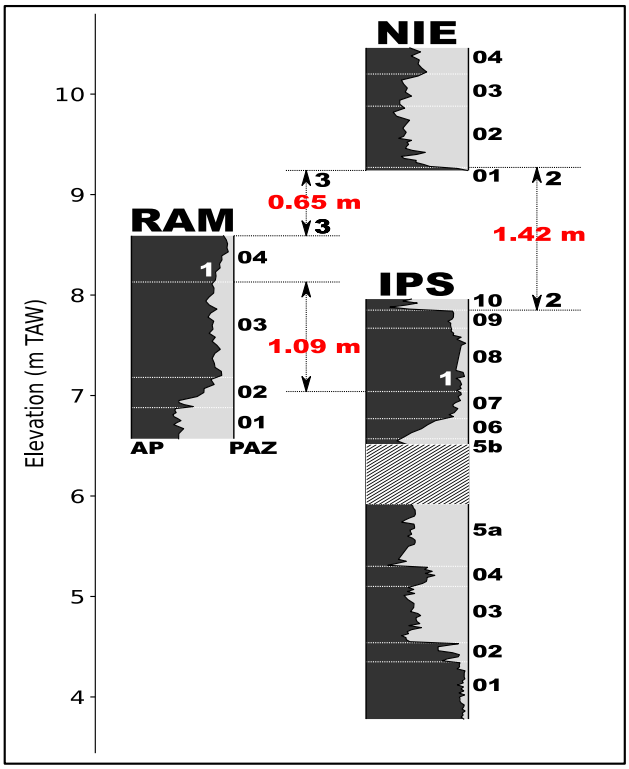

Fig. 5. Explanation of how IPS, RAM & NIE pollen diagrams (Figs. 3 and 4) are linked. No. 1 marks the point where *Carpinus* values rise and IPS is linked with RAM (1.09 m difference). No. 2 marks where IPS & NIE overlap: IPS-10 and NIE-01 are redundant (1.42 m difference). No. 3 marks the gap between late-temperate phase at top RAM and end of same interglacial cycle at base NIE (0.65 m difference). AP curves in black; PAZ = Pollen Assemblage Zones.

We assume NIE and IPS to slightly overlap where AP values decline (No. 2, Figs. 3 and 5), and therefore consider pollen zones NIE-01 and IPS-10 redundant (overlap). The same general palaeobotanical evolution stands out, though local disturbances by soil and/or slope processes (see Sections 4.2.1 and 4.2.3) hamper a detailed correlation. A 1.42 m gap separates the base of NIE-02 from the top of IPS-09 (Fig. 5), where we suppose these pollen diagrams to merge. This 1–1.5 m elevation difference between IPS and the other pollen sequences (RAM & NIE) is explained by differential compaction (Rieke and Chilingarian, 1974): IPS (Units 2–3) is much thicker than RAM and NIE (both only Unit 3)—we now refer to the complete sediment stacks (Fig. 2). More compaction in IPS means a lower position relative to RAM and NIE. The difference in thickness between the correlated pollen zones IPS-06 & 07 (47 cm) and RAM-02 & 03 (125 cm), both organic muds, supports this explanation (Fig. 5).

Finally, we assume that the interval between 8.59 (black line, Fig. 3) and 9.24 m TAW (0.65 m, No. 3, Figs. 3 and 5) allows for a continuous evolution from the late-temperate phase at the top of RAM to the end of the same interglacial cycle at the base of NIE. We therefore consider differential compaction sufficient—but necessary—to explain the observed differences in elevation. Other factors, such as river gradients, are considered less important in the case of distances of a few km at most: for example, Kiden (1991) estimated the gradient of the flood plain of the middle course of a typical lowland river (Scheldt, late-Holocene, pre-tidal) to be a

maximum of 15 cm/km. We therefore confirm our hypothesis that IPS, RAM & NIE belong to the same uninterrupted floodplain accumulation of a single interglacial complex.

5.2.2. IRN sequence

Fig. 3 shows the pollen diagram of an interglacial complex: two interglacial cycles (IPS)—the first is incomplete—and one interstadial (NIE) separated by colder intervals. In the following, we will refer to this composite diagram using the acronym IRN (**I**PS, **R**AM & **N**IE, right column Figs. 3 and 4), and name the two interglacial cycles in the IPS pollen diagram, Ipsvoorde (Ips) I (IPS-01 & 02) and Ipsvoorde (Ips) II (IPS-06 to 09), and the interstadial in the NIE diagram, Nieuwenrode (Nie) (NIE-04). The cold intervals are called Zenne (Zen) I (IPS-03 to 05) and Zenne (Zen) II (NIE-02 & 03), after the Dutch name of the nearby river.

5.3. Dating of the IRN pollen sequence

To date these organic deposits or, by extension, to establish during which interglacial complex—odd numbered marine isotope stage—meandering river activity resulted in *Units 2–3*, we first propose a broad time frame, narrow it down, and exclude other possibilities. Today, most European researchers accept that *in situ* shells of *Corbicula fluminalis* (***C***, Fig. 2) exclude an Eemian age (MIS 5e) for Units 2–3 and narrow the possibilities down to MIS 7, 9 or 11 (Keen, 1990; Meijer and Preece, 2000; Penkman et al., 2013). This hypothesis has been accepted in Belgium too (Bogemans, 2014). We can refine this crude estimation using archaeology (App. C2). Most of the 28 artefacts recovered from Bos van Aa pits II and III (Fig. 1B) are of flint and assumed to originally come from the same level (Unit 2, ▼, Fig. 2, Van Peer and Smith, 1990). Van Peer and Smith (1990) considered the lithic assemblage homogeneous and dominated by Levallois technology—no bifaces. The time when Levallois technology became a dominant and regular feature in stone artefact assemblages has conventionally been defined as the onset of the Middle Palaeolithic (Richter, 2011). Today, most European archaeologists agree (Hérisson et al., 2016) to place the transition from a Lower to a Middle Palaeolithic world between 300 and 250 ka (MIS 8, Lisiecki and Raymo, 2005), with a sudden rise in both the number of archaeological sites, and the use of Levallois technology during MIS 7 (see also Monnier, 2006). The combination of malacology (*C. fluminalis*) and archaeology (Levallois technology) therefore helps us to correlate Units 2–3 with MIS 7, IRN included.

Although Ips I & II (Fig. 3) resemble a typical Eemian vegetational development—similar tree taxa, especially *Carpinus*—the arrival of oak during a pre-temperate phase distinguishes Ips II from the Eemian (de Jong, 1988) in the Low Countries. Also Ips I cannot be correlated with the Eemian, because a succession of two interglacial cycles (Ips I & II) during the Last Interglacial complex (MIS 5) has never been observed in the Low Countries (Cleveringa et al., 2000; De Moor et al., 1978; Kasse et al., 2022; Zagwijn, 1961). The presence of 13 *Fagus* pollen grains in IPS (Fig. 3) and 1 in RAM (Fig. 4) supports this hypothesis: an inventory of Eemian terrestrial pollen sites nearby (1–40, blue dots, Fig. 6) yielded none in a total of 713 spectra (App. F). The presence of *Fagus* thus excludes either Ips I or II to be Eemian. Palaeobotany (*Fagus*) and malacology (*C. fluminalis*), in combination with archaeology (Levallois technology), therefore exclude that meandering river activity during the Last Interglacial complex (MIS 5) resulted in Units 2–3. Instead, the combination of proxies allows to correlate Units 2–3 with MIS 7.

If Units 2–3 correlate with MIS 7, we assume the second and youngest meandering river system (*Units 7–10*) to result from sedimentation during MIS 5. The Zemst North (ZEN) and Sint-Amands (SAM) pollen diagrams (Fig. 7) support this statement (Verbruggen, 1999 for a discussion; zonation scheme *cf.* Zagwijn, 1961). We plotted the SAM elevation range in Fig. 2 (red bar), though Sint-Amands locates outside the study area (No. 13, Fig. 6). We explain below how Unit 8 correlates with SAM.

According to Verbruggen (1999), SAM starts during the Eemian *Quercus-Corylus* pollen zone E4 and extends into the Herning stadial (EWI, MIS 5d, Behre, 1989), from which the upper diagram from Unit 10 (ZEN, red bar) continues, before developing into a local *Quercus* dominated Brørup interstadial (EWII, MIS 5c, Andersen,

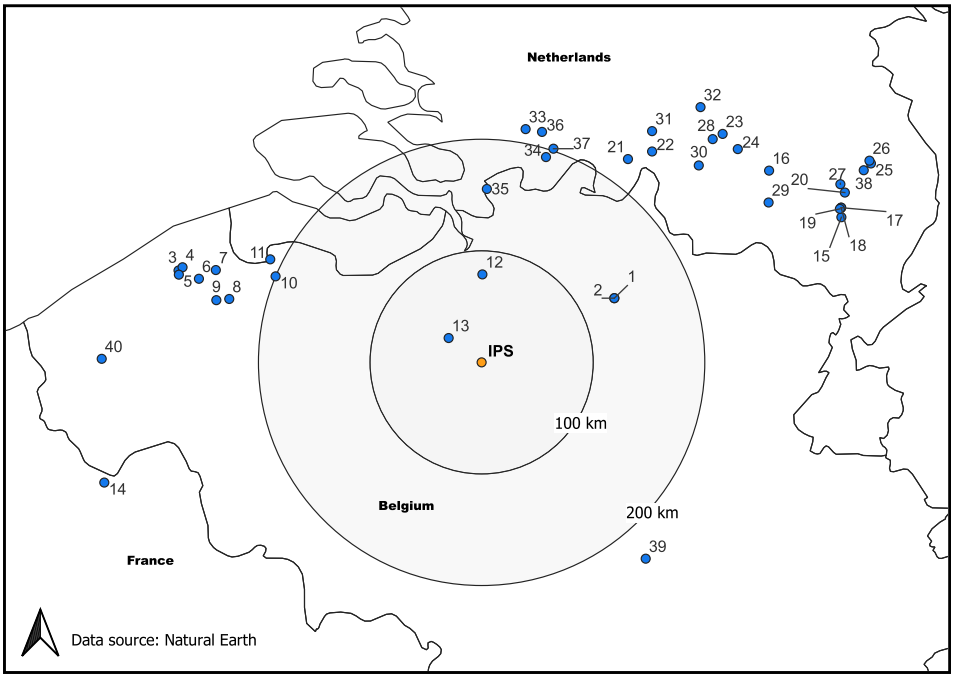

Fig. 6. Terrestrial sites with Eemian palynology (1–40, App. F), 100 km = diameter circle around IPS; figure demonstrates the absence of *Fagus* pollen around IPS.

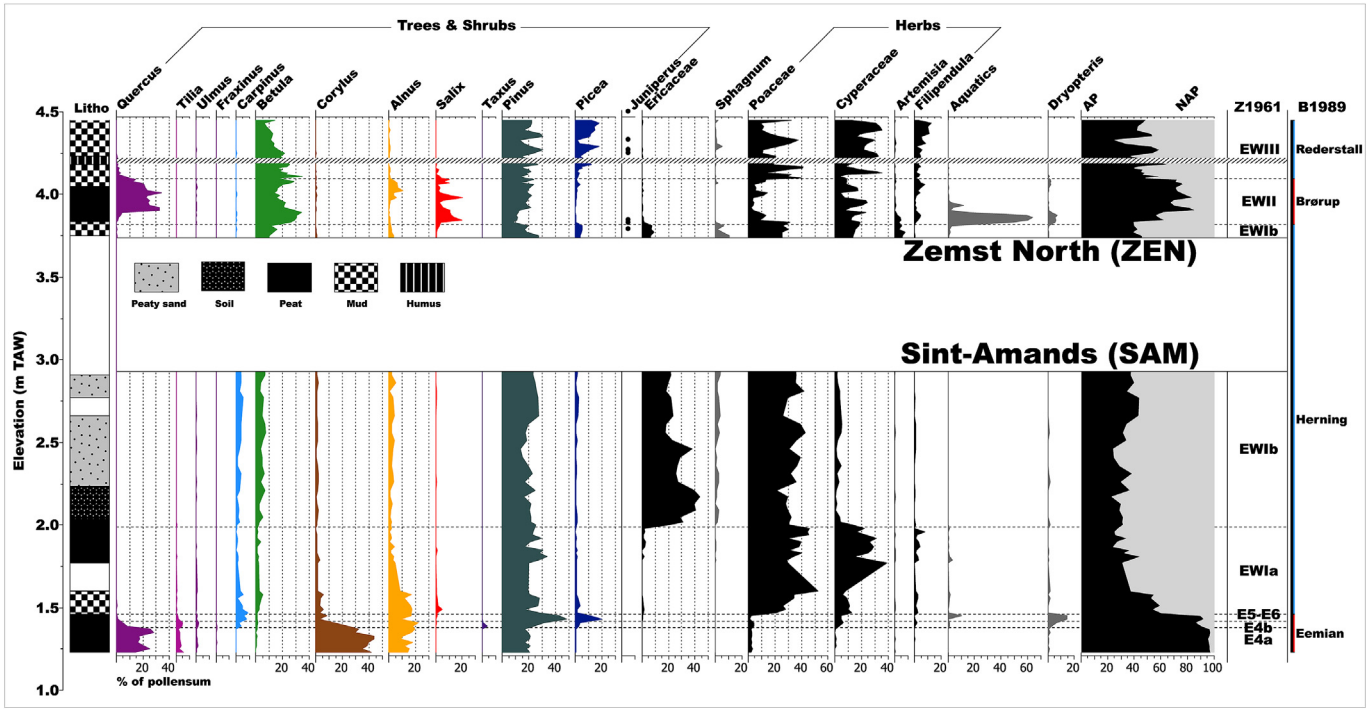

Fig. 7. Zemst North (ZEN) and Sint-Amands (SAM) percentage pollen diagrams (location see Figs. 1B and 2 and No. 13, Fig. 6) of selected taxa, curves in colour = AP (• presence *Juniperus* pollen), in black = NAP, in grey = excluded from pollen sum, spacing gridlines 10%, hatched = sterile, white space Litho column between 2.77–2.66 and 1.77–1.6 m TAW = core loss; ZEN & SAM combine to an incomplete MIS 5 sequence, Z1961 = zonation *cf.* Zagwijn (1961): Eemian interglacial (E4-E6), Herning stadial (EWI), Brørup interstadial (EWII), Rederstall stadial (EWIII) (B1989, Behre, 1989).

1961; Zagwijn, 1961). Van Overloop (*in* Bogemans, 1988) also suggested Brørup for Unit 10 (B222, red •, Fig. 2). Similar accumulative sequences from two more seaward sites have been found in different paleo-morphological positions: Moershoofde is an infill—mostly gyttja—of a former Eemian tidal gully, above which a Brørup peat layer developed (No. 11, Fig. 6, Zagwijn, 1961); the pollen diagram of Beernem-Mouton, however, was sampled in a tributary valley close to the Eemian coastline (No. 8, Fig. 6, Chenopodiaceae present, De Moor et al., 1978). The elevation (*c.* 1.25 m TAW) and pollen zone (E4a) at which peat formation started in Beernem-Mouton and SAM are the same, though Sint-Amands is 100 km more inland (No. 13, Fig. 6). Such a synchrony in a lowland demands permanently high groundwater levels under close marine influence. An Eemian sea level reconstruction based on pollen data from tidal flats (nos. 3–7, Fig. 6, Mostaert and De Moor, 1984; Mostaert and De Moor, 1989) suggests indeed that highest mean uncorrected sea level during pollen zone E4b oscillated around 0–1 m TAW, and that the sea, compared with the Holocene, penetrated deeper into the land (De Clercq et al., 2018). We therefore correlate an eventual pollen record from the lower organic Unit 8 (especially from B195) with SAM, at only 14 km. ESR age estimates on a mammoth molar from Units 4–5 (assemblage Zemst IIB, Germonpré, 2003) produced the following *terminus post quem* for Unit 8: 126.2 ± 9.3 ka (early U-uptake model) or 131.9 ± 7.8 ka (linear U-uptake model) (Germonpré et al., 1993). These results within error margins also suggest correlation of Unit 8 with the Eemian interglacial (130–115 ka, Lisiecki and Raymo, 2005).

Units 7–10 thus result from meandering river activity during the greater part of the Last Interglacial complex (MIS 5e-b), during which low-energy marshy fluvial conditions without major erosional events prevailed in Northwest European lowlands (Mol et al., 2000; van Huissteden et al., 2001). Quite similar environmental conditions must have prevailed during MIS 7, as during both interglacial complexes climate oscillations forced a similar set of tree taxa to expand and retract their ranges. The resulting pollen assemblage zones may look similar, but differ in age and detail (homotaxis *cf.* Bowen, 1978)—*e.g.*, arrival time and relative abundance of individual taxa. Homotaxis or homotaxy (North American Commission on Stratigraphic Nomenclature, 2005) necessitates the use of other criteria or proxies to establish the age of the pollen record. Elevation is of prime importance for distinguishing pollen records from river terrace aggradations (Turner, 1989). The similarity between the Brørup in ZEN (Fig. 7) and the Nieuwenrode interstadial in NIE (Fig. 3), an elevation difference of 6 m (Fig. 2), illustrates homotaxy. Brørup look-alikes are not uncommon. For example, Zagwijn (1973) compared the Bantega interstadial to the Brørup. Both the Bantega (No. 4, Fig. 1C and de Jong, 1988) and Nieuwenrode interstadials correlate with part of MIS 7 and might be synchronous (MIS 7a?, Fig. 8).

Units 4–5 represent braided river deposits bound to the southwest by a MIS 7 meandering channel belt (Units 2–3) and to the northeast by a similar single thread system from the last interglacial complex (Units 7–10) (Fig. 2). Units 4–5 are therefore younger than MIS 7 and older than MIS 5, and hence date from MIS 6 (191–130 ka, Lisiecki and Raymo, 2005): a conclusion supported by Lister and Sher (2001) and the just-mentioned ESR age estimates (see Units 7–10). The paleosol that developed in the lag deposit (Unit 6, Fig. 2) is correlated with the Eemian Rocourt soil (Gullentops, 1954; Gullentops et al., 2001). The top of Unit 6 indicates the ground level during the Eemian, about 5 m lower than current topography.

Units 11–12 are younger than the Brørup interstadial from Unit 10, above which a coarse sediment truncates the MIS 5 accumulation. Mol et al. (2000) and van Huissteden et al. (2001) situate this erosional event during MIS 4. The remainder of Units 11–12 must then date from MIS 3–2. Zagwijn and Paepe (1968) and Bogemans (1988) correlate the widespread gravel string near the top of Unit 11

(■■■) with the Dutch Beuningen Gravel Bed, which formed during the Late Pleniglacial (MIS 2, *c.* 28–18 ka cal B.P., Kasse, 2002). We correlate the fluvio-aeolian deposits of Unit 11 with both the Middle to Late Pleniglacial (MIS 3–2) aeolian Tisselt Member of the Gent Formation (Beerten et al., 2017)—which has its stratotype in the study area—and the fluvial Lembeke Member of the Zemst Formation (Bogemans, 1993, 1996).

Unit 12 is younger than the Beuningen Gravel Bed and dates from the Late Pleniglacial-Lateglacial transition (*c.* 14.7/14.0 ka cal B.P., Kasse, 2002) when river morphology changed from a braided into a single straight incised channel—hence 'transitional rivers' (Vandenberghe and Woo, 2002). Wind picked up sand grains from the abandoned floodplain and built low sand ridges along all major Flemish rivers. These ridges are called 'kouter' or 'windwal' in Flanders (Gullentops et al., 1981). We correlate Unit 12 with the MIS 2 aeolian Opgrimbie Member of the Gent Formation (Beerten et al., 2017). Finally, a Holocene soil (MIS 1) has developed in the top deposits (Units 11–12).

5.4. A critical appraisal of the current river evolution model: the Balderton Terrace

Except for the hitherto unpublished pollen data (IRN), we reinterpreted earlier observations made by other workers. The result is a river evolution model that runs counter to current opinion (Bogemans, 1993; Heyse and Demoulin, 2018). In the following, we therefore explain, situate, and criticize the current model.

The pre-Eemian age of IRN, however, has never been questioned. Since their partial presentation (RAM & NIE, Verbruggen, 1982), Verbruggen (1999) and Bogemans (1993) have considered these pollen data samples of (a) Saalian Stage river terrace(s). From borehole B243 and north-eastwards (Figs. 1B and 2), however, opinions differ. Bogemans (1988) and Gulinck et al. (1971) interpreted all observations from boreholes and excavations in this area as the result of continuous fluvial and aeolian activity during the Late Pleistocene (Paepe, 1972). Their conclusions conformed to the theoretical framework, which goes back to the ideas of Tavernier (1954). Tavernier eventually launched *Corbicula fluminalis* as an Eemian index fossil, which frequently occur in basal deposits of the Scheldt basin (*e.g.*, De Moor and Lootens, 1975; Halet, 1933; Rutot, 1910). De Moor (1963) and Paepe (Paepe and Vanhoorne, 1967) modified and extended Tavernier's model, but took for granted the status of *C. fluminalis* as an Eemian index fossil. Bogemans (1988, 1993) conformed her observations in the Bos van Aa pits (Fig. 1B) to the prevailing stratigraphical framework, which she confirmed through findings of abundant bivalved *C. fluminalis* in basal deposits. Other proxies seemingly supported the Eemian and Weichselian Early Glacial age (MIS 5) of most of the Bos van Aa deposits (Germonpré et al., 1993; Van Peer and Smith, 1990). We, however, have questioned these conclusions since opinions changed about the chronostratigraphic value of *C. fluminalis* (Keen, 1990; Meijer and Preece, 2000; Penkman et al., 2013), the introduction of Levallois technology (Hérisson et al., 2016), and mammoth remains (Lister, 2022; Lister and Sher, 2001, see further). Bogemans (2014) accepted the late Middle Pleistocene age of sites with *C. fluminalis* and, in the following, we reassess the archaeology (Van Peer and Smith, 1990) and palaeozoology (Germonpré et al., 1993) of Bos van Aa, and correlate this site with the Balderton Terrace in the English East Midlands (Brandon and Sumbler, 1991).

Van Peer and Smith (1990) classified the artefacts from Bos van Aa as typical Mousterian because of the preponderance of Levallois technology and the absence of bifaces (Turq, 2000). This Mousterian classification, however, does not exclude a pre-Eemian age for this site. Similar lithic industries (Hérisson et al., 2016) have been discovered at, for example, Biache-Saint-Vaast (No. 2, Fig. 1C, Tuffreau and Sommé, 1988) and Maastricht-Belvédère (No. 1, Fig. 1C, Roebroeks, 1988). Both sites contain *C. fluminalis*—and abundant *Fagus* pollen in Biache—and correlate with MIS 7 (Bahain et al., 2015; Van Kolfschoten and Roebroeks, 1985; Vandenberghe et al., 1993).

Germonpré et al. (1993) further invoked osteometric data (index values) from supposedly woolly mammoth (*Mammuthus primigenius*) molars to support a Weichselian Early Glacial age for the Bos van Aa assemblage Zemst IIB (Units 4–5, Fig. 2). The calculated index values are, however, between mean values (Maglio, 1973) for early Middle Pleistocene steppe *M. trogontherii* and late Middle to late Pleistocene woolly mammoth *M. primigenius* (Lister and Sher, 2001). It is hard to maintain that the molar data came from a pure breed of *M. primigenius*. Instead, they suggest a bimodal distribution. Lister (2022, Fig. 28) recently confirmed this assumption by comparing mammoth molar data from the Balderton Sand and Gravel (see further) with the assemblage Zemst IIB (Germonpré, 2003). He concluded that they both conform to a mixture of 'primigenioid' and 'trogontherioid' morphologies. He ascribed this pattern to an admixture of MIS 7 interglacial with MIS 6 braided river deposits and placed the final transition to *M. primigenius* near the MIS 7-6 boundary. We indeed demonstrated considerable reworking of Units 2–3 (MIS 7) during sedimentation of Unit 4 (MIS 6) (BAN: ***h***; ZSL: ***M***, red bar, green bar and •, and brown bar; B232: ***h*** and brown •), and suggested *in situ* mammoth remains in Unit 2 (BAS, ***M***) (Fig. 2). Also, the composition of the assemblage Zemst IIB proves mixing: the Big Four of the cold and arid mammoth steppe (Guthrie, 2001) predominate—mammoth, woolly rhinoceros, horse, and (steppe) bison (App. C5)—but with an admixture of warm climate species from assemblage Zemst A (Unit 2). We may even propose assigning most of these mammal remains to Units 2–3 (see also Scott and Buckingham, 2021). The palaeobotanical evolution during MIS 7 (IRN) allows mammals with divergent ecological and climatological preferences to intermingle in a typical MIS 7 fossil assemblage. We demonstrated the evolution from a temperate forest (Ips I) to a mammoth steppe (Zenne I) and back to a temperate forest (Ips II) that degraded into a forest steppe (Zenne II), in which oak returned (Nie). Although Germonpré et al. (1993) qualified the assemblage Zemst IIB as steppe-like, it has all but one mammalian taxa in common with the MIS 7c-a assemblage of Schreve (2019), in which steppe (*M. trogontherii*) and woolly mammoth (*M. primigenius*) coexist with interglacial straight-tusked elephant (*Palaeoloxodon antiquus*)—present in assemblage Zemst A (Germonpré, 2003). Only reindeer (*Rangifer tarandus*) is missing in Schreve's MIS 7c-a assemblage, but is abundant in Bos van Aa (App. C5). Lister and Brandon (1991), however, described reindeer remains from the MIS 6 Balderton Sand and Gravel. Evidently, mixing of MIS 6 with MIS 7 fossil assemblages occurred in Bos van Aa.

Bridgland et al. (2014) also demonstrated mixing in the just-mentioned Balderton Sand and Gravel, the principal deposit of the Balderton Terrace, which marks a former course of the English river Trent (No. 3, Fig. 1C, Brandon and Sumbler, 1991). Apart from the above-mentioned mammoth molar morphology and other mammal remains (App. C5), the Balderton Terrace and Bos van Aa have more proxies in common. For example, ESR age estimates on mammoth molars overlap, and both the Balderton Sand and Gravel and Units 4–5 correlate with MIS 6 (Grün *in* Brandon and Sumbler, 1991; Germonpré et al., 1993). The lithostratigraphy also matches—compare Brandon and Sumbler (1991) with Fig. 2 (this study). In the cold climate Balderton Sand and Gravel, Brandon and Sumbler (1991) recognized a fossiliferous lower bed (= Unit 4, Fig. 2) and a more sterile upper one (= Unit 5), in a generally upward fining sequence separated by an erosion horizon. At the top of

both sediment stacks, signs of a standstill occur with aeolian activity followed by soil processes (Unit 6b). The only difference is the near absence in the Balderton Terrace of an equivalent of the Pleniglacial (fluvio-)aeolian Units 11–12. Also, below the Balderton Sand and Gravel, the fossil content of MIS 7 river channels matches with Units 2–3: Bridgland et al. (2014) recorded both *C. fluminalis* and *Fagus* pollen from interglacial deposits in the Balderton Terrace. Apparently, climatic conditions in England and Belgium during MIS 6 & 7 resulted in a similar river evolution, which offers opportunities for future correlations between these regions in that time frame.

5.5. Land-sea correlation: ODP 980 and MD01-2447 (Fig. 8, Table 1)

The MIS 7 pollen record is compared to climate oscillations recorded in oxygen isotope ($\delta^{18}O$) data. We use planktic foraminiferal $\delta^{18}O$ data from Ocean Drilling Program (ODP) site 980 in the North Atlantic Ocean ~400 km off the Irish NW coast (55°N, No. 5, Fig. 1C, McManus et al., 1999) and deep-sea core MD01-2447 ~100 km off the Spanish Galician coast (42°N, No. 6, Fig. 1C and Desprat et al., 2006). Planktic $\delta^{18}O$ values are influenced by the temperature and $\delta^{18}O$ of ambient seawater (McManus et al., 1999), and are therefore most suitable to compare to a terrestrial pollen record such as IRN. MD01-2447 has the advantage of providing a direct land-sea correlation through its pollen record. To establish a tentative chronological framework, we tuned IRN (AP, *Quercus*, and *Juniperus* composite curves) to the MD01-2447 pollen record using pollen zone boundaries as control points (6 vertical dotted lines IRN, Fig. 8 (A)) according to the age-depth model of Desprat et al. (2006). Obviously, there may have been time lags between the vegetation development in the Low Countries and north-western Iberia—as has been shown for MIS 5 (Sánchez Goñi et al., 2005)—but we intend to demonstrate the similarity (or difference) between the succession and amplitude of IRN and MD01-2447 climate oscillations. We selected MD01-2447 pollen percentage curves of temperate and humid forest taxa (red line, Fig. 8 (B)) and ubiquist plants (blue line) as proxies for north-western Iberian warm and cold climate oscillations (Desprat et al., 2006).

The IRN pollen record extends roughly between 190 and 240 ka BP (Fig. 8) and covers all marine isotope substages (Railsback et al., 2015), although some only partially (MIS 7a & e). The MD01-2447 and ODP 980 MIS 7 planktic $\delta^{18}O$ curves (Fig. 8 (C) and (D)) show two asymmetric periods with light(er) values (MIS 7e and MIS 7c-a) separated by an interval lasting *c.* 15 ka with heavy $\delta^{18}O$ values (MIS

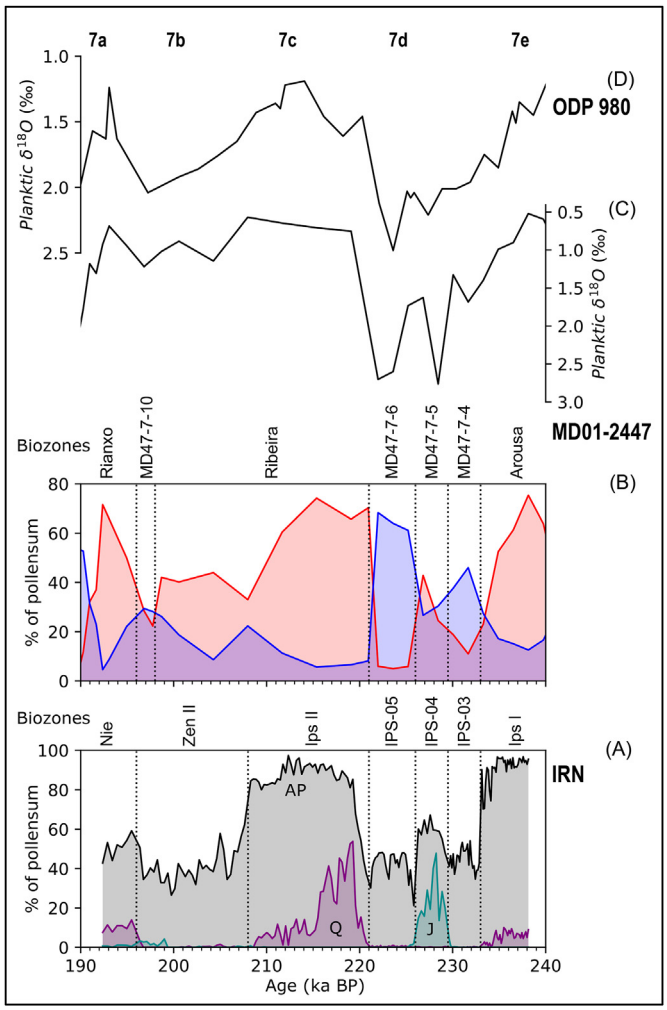

Fig. 8. MIS 7 land-sea correlation: (A) IRN Arboreal Pollen (AP), *Quercus* (Q), and *Juniperus* (J) pollen percentage composite curves, constructed from Fig. 3 dataset (colours are alike) after removal of redundant pollen zones IPS-10 and NIE-01 (see Section 5.2), and tuned (linear interpolation) to the Desprat et al. (2006) age-depth model using pollen zone boundaries as control points (6 vertical dotted lines); (B) MD01-2447 pollen percentage curves of temperate and humid forest taxa (red line) and ubiquist plants (blue line); (C) MD01-2447 planktic $\delta^{18}O$ curve; (D) ODP 980 planktic $\delta^{18}O$ curve (McManus et al., 1999); (B), (C), and (D) according to Desprat et al. (2006); Biozones see Table 1, MIS 7 substage lettering (7a-e) according to Railsback et al. (2015).

Table 1
IRN (Fig. 3) versus MD01-2447 pollen zonation and vegetation formation; MD01-2447 data adapted from Desprat et al. (2006).

IRN			MD01-2447		
Pollen zones	*Vegetation formation*	*Superzones*	*Pollen zones*	*Vegetation formation*	*Superzones*
NIE-04	Oak-birch forest steppe	Nieuwenrode	MD47-7-11	Oak-beech-hornbeam forest	Rianxo
NIE-03	Birch-pine forest steppe	Zenne II	MD47-7-10	Open oak forest with beech and hornbeam and with heathland or dry grassland	
NIE-02	Pine-birch forest steppe		MD47-7-9	Open beech-oak forest with hornbeam	Ribiera
IPS-09	Pine-birch taiga	Ipsvoorde II	MD47-7-8	Oak forest with beech and heathland	
IPS-08	Oak-hornbeam forest				
IPS-07	Mixed-oak forest		MD47-7-7	Beech-oak-hornbeam forest	
IPS-06	Open oak-birch-pine forest				
IPS-05	Mammoth steppe or steppe tundra with birch	Zenne I	MD47-7-6	Dry grassland	
IPS-04	Open juniperus-birch vegetation		MD47-7-5	Open oak forest	
IPS-03	Boreal wetland		MD47-7-4	Heathland and grassland with birch and oak	
IPS-02	Pine-spruce taiga	Ipsvoorde I	MD47-7-3	Oak forest with hornbeam, birch, and heathland	Arousa
IPS-01	Oak-hornbeam forest				

7d). The youngest and longest phase is, in turn, a complex that consists of two unequal periods with light values (MIS 7c & a) and an interval with lower sea surface temperatures (MIS 7b). Ninkovich and Shackleton (1975) first demonstrated the bipolar character of MIS 7, with continental ice sheets attaining 80% of their maximum size during MIS 7d. This made Bowen (1978) question whether MIS 7c-a and 7e 'ought not be recognized as separate interglacials', which is also the opinion of Past Interglacials Working Group of PAGES (2016).

This 'interglacial-to-glacial-to-interglacial oscillation' (Ruddiman et al., 1977) is also recorded in the IRN Ips I-Zen I (IPS-03 to 05)-Ips II succession (Fig. 8 (A)), which, at 51°N, shows the botanical evolution of an oak-hornbeam forest (IPS-01) to a steppe tundra (IPS-06) and back to an oak-hornbeam forest (IPS-08) in only 3 m of organic mud, clay, and peat (Table 1, Fig. 3). We confirm the earlier suggestion of two woodland stages during MIS 7 in current temperate climate regions (Candy and Schreve, 2007). The contemporaneous vegetation at 42°N (MD01-2447) consists of the same forest (MD47-7-3)-steppe (MD47-7-6)-forest (MD47-7-8) succession, but with the dominance of beech over hornbeam in north-western Iberia from the Ribeira forest phase onwards (Table 1, Desprat et al., 2006). The (abundant) presence of *Fagus* pollen contradicts with its near absence during MIS 5 in the same area (Sánchez Goñi et al., 2005), which supports our *Fagus* hypothesis (Fig. 6). The coming and going of forest, however, is not so straightforward as the simple 'interglacial-to-glacial-to-interglacial' notion. In the middle of MIS 7d, lighter planktic $\delta^{18}O$ values, increasing values of temperate and humid forest taxa (MD47-7-5), and the rise and fall of *Juniperus* (IPS-04) indicate a brief (*c.* 3.5 ka), but nevertheless pronounced warming (Fig. 8).

The younger half of MIS 7 (MIS 7c-a) is even more complex. The IRN Ips II-Zen II-Nie succession first develops into an oak-hornbeam climax vegetation (IPS-08), after which it rapidly degrades into a pine-birch forest steppe (NIE-02 & NIE-03), in which oak returns (NIE-04) (Table 1). Although MD01-2447 shows the same evolution from a closed to a more open vegetation with declining tree values, the Ribeira oak-beech-hornbeam forest resisted the climate deterioration from 208 ka BP onwards (Table 1, Fig. 8 (B)). This difference between the IRN and MD01-2447 vegetation composition during MIS 7c-a results in different pollen zone boundaries: Desprat et al. (2006) extend the Ribeira forest phase to 198 ka BP despite the obvious lower values of temperate and humid forest taxa from 208 ka BP onwards. At 51°N (IRN), however, the climate deterioration was severe enough to push temperate trees out of Flanders (AP drops) and end the warm Ipsvoorde II period (Fig. 8 (A)). During MIS 7a a closed oak-beech-hornbeam forest rapidly restored in north-western Iberia (Rianxo), while only oak could reach Flanders (Table 1). Especially the ODP 980 planktic $\delta^{18}O$ curve suggests that lack of time, rather than climatic conditions, prevented the arrival of temperate trees other than oak during the Nie interstadial (Turner, 1998).

There is a good match between the ODP 980 (planktic $\delta^{18}O$) and MD01-2447 (planktic $\delta^{18}O$ and pollen) curves on the one side, and IRN on the other, despite the expected, but nevertheless interesting latitudinal differences. This match allows to correlate IRN down to marine isotope substage level and to use this pollen sequence as a correlation tool in future attempts to develop a solid Saalian Stage palynostratigraphy.

5.6. Correlation between IRN and Southern European pollen sequences (Table 2, Fig. 1C)

We refer to the caption of Table 2 for site-related references and Fig. 1C for the location of the sites.

5.6.1. Correlation table

In Table 2, we correlate forest phases recorded in Southern European pollen sequences and IRN with MIS 7 stratigraphy. Lake Kopais is our reinterpretation of the original based on a correlation with the Ioannina-284 and Tenaghi Philippon pollen sequences. We consider the combination of two oak forest phases (KP 5 & 7) separated by a grassland dominated interval (KP 6), below the Eemian zone KP 9a, to represent MIS 7 in Lake Kopais. The colder MIS 7b interval (see Section 5.5) is not reflected in the Lake Kopais pollen diagram during zone KP 7 and barely noticeable in the Ioannina-284 AP curve (zone G-3a). In the latter, the distinction between the Zitsa II (MIS 7a) and Zitsa III (MIS 7c) forest phases could only be made because of the expansion in the lowland and mountains around Lake Ioannina of late temperate tree taxa (*Carpinus*, *Abies* and *Fagus*) that induce a double peak of *Quercus*. Hornbeam, fir and beech were absent during MIS 7 in the oak-dominated lowland surrounding Lake Kopais. In the Tenaghi Philippon sequence, palynologists counted only 7 spectra (24 cm interval) with AP values < 50% between 198.82 and 200.7 ka (MIS 7b), which could easily be overlooked with the 60 cm sampling resolution of Lake Kopais (Table 2). We further support the propositions of Reille et al. (1998; *contra* Tzedakis et al., 1997) and Desprat et al. (2006) to correlate, respectively, only the first part of Roma III (VdC-7a, Valle di Castiglione) and the second part of zone H2 Symvolon (Tenaghi Philippon) with MIS 7a (Table 2).

Table 2
Correlation between MIS 7 warm intervals and forest phases recorded in Southern European pollen sequences and IRN. Elevation of the top of the drilling in metres above sea-level (m asl), Morphology refers to the origin of the depression in which organic deposits accumulated, Resolution is sampling distance expressed in cm, Mid-7d-warming(w), – means unrecorded. Lac du Bouchet (Reille et al., 1998, 2000), MD01-2447 (Desprat et al., 2006), MD01-2443 (Roucoux et al., 2006; Tzedakis et al., 2004), Valle di Castiglione (Follieri et al., 1988, 1989), Lake Ohrid (Sadori et al., 2016, Masi et al., 2016; Sadori et al., 2018), Tenaghi Philippon (Koutsodendris et al., 2023a, 2023b; Wijmstra and Smit, 1976), Ioannina-284 (Roucoux et al., 2008) & Lake Kopais (Okuda et al., 2001).

Site	IRN	Lac du Bouchet	MD01-2447	MD01-2443	Valle di Castiglione	Ohrid	Tenaghi Philippon	Ioannina	Kopais
Elevation (m asl)	15	1200	−2080	−2925	44	693	40	473	95
Morphology	Floodplain	Crater	Marine	Marine	Crater	Tectonic	Peatland	Tectonic	Polje
Resolution (cm)	2–5	<5 to 10	5–10	2–8	20–25	64	2–6	20	60
MIS	*Local names of forest phases*								
7a	Nieuwenrode	Bouchet 3	Rianxo	Belem	VdC-7a	OD-6	Second part H2 Symvolon	Zitsa 3	KP 7
7c	Ipsvoorde II	Bouchet 2	Ribiera	Cascais	Roma II		H1 Symvolon	Zitsa 2	
Mid-7d-w	IPS-04	Pinus peak Belvezet?	MD47-7-5	–	VdC-4b	–	225.96–228.25 ka	G-7a?	–
7e	Ipsvoorde I	Bouchet 1	Arousa	Estoril	Roma I		Strymon	Zitsa 1	KP 5a-b

5.6.2. MIS 7 vegetation dynamics and climate variability

Across Europe, mainly deciduous mixed-oak woodland thrived during the first half of the MIS 7 warm phases (MIS 7e, c & a), after which *Carpinus betulus* mostly accompanied *Quercus* spp. in the lowlands. Hornbeam, however, is near absent in the two most southern sequences Lake Kopais and MD01-2443. Heathland (Ericaceae) was also present during forest phases along the wet Atlantic coast of the Iberian Peninsula (MD01-2443 & 2447). Pollen sequences from Southern European sites surrounded by hilly or mountainous regions demonstrate sometimes very high values of *Fagus* and/or *Abies* (Valle di Castiglione, Lake Ohrid & Ioannina-284), whereas spruce grew in more northern low- and highlands (IRN & Lac du Bouchet). Pinus can sometimes reach such high values—natural (Lake Ohrid) or taphonomic (MD01-2443 & 2447) overrepresentation—that it was left out of the pollen sum. During cold intervals (MIS 7d & b), steppe plants and grassland dominated (*Artemisia*, Caryophyllaceae, Chenopodiaceae & Poaceae), and in moister regions (MD01-2443, MD01-2447 & IRN), also heathland expanded.

There are many similarities between climate variability in Northwest European lowlands (IRN) and Southern Europe as deduced from the vegetation dynamics in the pollen sequences: first, an abrupt cooling followed by unstable but rapidly deteriorating climatic conditions at the end of MIS 7e; second, a threefold division of the next cold interval (MIS 7d) in a mostly wetter, cold first part, followed by a short, but important warming, ending with the coldest and driest interval; third, the re-expansion of a more open (forest-)steppe vegetation during a short and minor cooling (MIS 7b).

An abrupt cooling at the end of MIS 7e. At the end of Ipsvoorde I (IPS-01), values of most temperate forest tree taxa suddenly decrease while *Pinus* and *Betula* increase, after which AP values shortly fluctuate before they drop 50% over only a 2 cm interval (1 spectrum) at the end of IPS-02 (Fig. 8). Such an abrupt temperate forest contraction and a subsequent drop of the AP values have also been recorded in Lac du Bouchet, MD01-2443, MD01-2447, Valle di Castiglione (isolated Caryophyllaceae peak before the end of VdC-5), Tenaghi Philippon (AP drops from 80 to 15% over a 4 cm interval (1 spectrum) at *c*. 230 ka), and Ioannina-284. The sudden decline of temperate forest tree populations is obviously real (*contra* Reille et al., 1998) and points to an abrupt cooling and subsequent unstable but rapidly deteriorating climatic conditions at the end of MIS 7e. Probably due to the lower sampling resolution, it was not recorded in Lake Ohrid and Lake Kopais (Table 2).

A threefold division of MIS 7d and the Mid-MIS 7d-warming. The following cold interval in IPS (Zenne I, Fig. 8) starts with a cold, wet first part (IPS-03) with the development of a boreal wetland (Ericaceae and *Sphagnum*), and ends cold and dry (IPS-05) with extensive grassland (Poaceae). In between, however, is a brief, but important Mid-MIS 7d-warming (IPS-04): the rise and fall of *Juniperus* covers only a 20 cm interval (10 spectra). On the Atlantic coast of the Iberian Peninsula (MD01-2443 & 2447), heathland also peaked first after which it was replaced by dry grassland between 226–221 ka in MD01-2447, but not before this cold phase was interrupted by a warm fluctuation (MD47-7-5), marked by a re-expansion of oak woodland. The Mid-MIS 7d-warming, however, does not seem to be reflected in the MD01-2443 diagram. Increased aridity was recorded during the Belvezet stadial of Lac du Bouchet, but without a clear warming, except for the lowest *Pinus* peak accompanied by somewhat higher values of temperate forest trees. In the Valle di Castiglione sequence, an important forest re-expansion (VdC-4b) occurred during the middle of a cold, dry phase, which did not seem to be wetter at first. Wetter conditions (Cyperaceae peak), however, did precede a drier phase with steppe plants in Tenaghi Philippon. The very distinct warm fluctuation in between is dated to *c*. 226–228 ka (28 cm interval). In the Ioannina-284 sequence, the second of two cold zones during MIS 7d appeared drier than the first (*Artemisia* and *Ephedra* more abundant). Zone G-7a probably correspond to the Mid-MIS 7d-warming with a *Quercus* re-expansion and lower *Artemisia* values at *c*. 230 ka. Probably due to the lower sampling resolution it was not recorded in Lake Ohrid and Lake Kopais (Table 2). In pollen sequences with higher resolutions (IRN, MD01-2447, Valle di Castiglione & Tenaghi Philippon), however, the Mid-MIS 7d-warming is clearly present. Depending on the site-specific age-depth model it is in the interval 230–225 ka, but lasted only 2–3 ka (Tenaghi Philippon). This is the first millennial-scale Saalian Stage climate fluctuation that has been demonstrated on a supra-regional scale.

A minor and short-lived cooling during MIS 7b. During the cold Zenne II interval of IRN (Fig. 8), stable *Pinus* and *Betula* values combined with substantial Poaceae and Cyperaceae pollen demonstrate a forest-steppe vegetation. A reduction of the forest in favour of more open vegetation was also recorded during the short (10 cm interval, 4 spectra) Bonnefond stadial in Lac du Bouchet. The fact that MIS 7b was not recorded in Lake Kopais, barely noticeable in the Ioannina-284 AP curve and only of short duration in Tenaghi Philippon (see Section 5.6.1) supports the hypothesis that cooling must have been minor. Strong disagreement about the duration of the preceding warm forest phase (MIS 7c: MD01-2443 10.3 ka, IRN ~13 ka, Ioannina-284 ~16ka, and MD01-2447 ~23 ka) and the instantaneous expansion of all tree taxa without a clear pioneer succession at the start of MIS 7a (Lac du Bouchet, MD01-2443, MD01-2447, Valle di Castiglione & Ioannina-284), reinforces the notion of only a minor and short-lived cooling during MIS 7b.

6. Conclusions

1. Well-preserved floodplain deposits dating from the penultimate interglacial complex (MIS 7) occur in the subsurface of an area to the north of Brussels (Belgium). We demonstrated that the combination of multiple proxies (*Corbicula fluminalis*, Levallois artefacts, *Fagus* pollen, and remains of both steppe and woolly mammoth) is a strong predictor for MIS 7 river activity.
2. Only high resolution pollen sequences from the same area allow for a distinction between MIS 5 and MIS 7 vegetation dynamics in a fluvial setting. The elevation at which homotaxial pollen sequences occur must match or fit into a local river evolution model before the related organic deposits be considered contemporaneous.
3. Pollen samples from a MIS 7 floodplain combine to the IRN pollen sequence spanning two interglacial cycles (MIS 7e & c) and one interstadial (MIS 7a) separated by colder intervals (MIS 7d & b). We convincingly curve-matched IRN down to marine isotope substage level.
4. MIS 7 vegetation dynamics and climate variability show many similarities across Europe: an abrupt temperate forest contraction marking a sudden cooling at the end of MIS 7e; a threefold subdivision of MIS 7d in a cold, wet start with heathland and a cold, dry end with steppe plants, with a short, but substantial warming in between during which woodland re-expanded; a minor and short-lived cooling during MIS 7b with the development of a forest-steppe vegetation.
5. The Mid-MIS 7d-warming is the first millennial-scale Saalian Stage climate fluctuation that has been demonstrated on a supra-regional scale. It situates roughly between 230–225 ka, but lasted only 2–3 ka.
6. Given the presented multi-proxy supported river evolution model and correlation with marine isotope and Southern European long pollen records, we convincingly demonstrated that IRN represents the palynological fingerprint of climate

variability during the penultimate interglacial complex in Northwest European lowlands. The IRN pollen sequence serves as a basis for eventual future attempts at developing a solid Saalian Stage palynostratigraphy.

Author contributions

Filip Van Beirendonck: Conceptualization, Methodology, Data curation, Writing – original draft, Visualization; **Nathalie Van der Putten:** Writing – review & editing; **Cyriel Verbruggen:** Investigation, Resources, Writing – review & editing, Supervision.

Declaration of competing interest

The authors declare that they have no known competing financial interests or personal relationships that could have appeared to influence the work reported in this paper.

Data availability

We have shared all relevant data in the Supplementary Material section. Other data will be made available on request.

Acknowledgments

We deeply appreciate the time and effort Kees Kasse made for commenting and correcting an earlier version. We acknowledge Jef Vandenberghe for the many helpful comments and suggestions that greatly improved the final draft. Jeroen Schokker, Delia Oppo, Stéphanie Desprat and Donatella Magri made available, respectively, the TNO, ODP 980, MD01-2447 and Valle di Castiglione data. What would we do without good data! We also would like to thank Kate Scott for improving our prose, Jeannine Aters for her hospitality, and last but not least, Adrian Lister for being a beacon of open-mindedness. It has been one hell of a ride. Thanks to all.

This research did not receive any specific grant from funding agencies in the public, commercial, or not-for-profit sectors.

Appendices A-F. Supplementary data

Supplementary data to this article can be found online at https://doi.org/10.1016/j.quascirev.2023.108113.

References

Andersen, S.T., 1961. Vegetation and its environment in Denmark in the early Weichselian glacial (last glacial). Danmarks Geologiske Undersøgelse II. Række 75, 1–175.
Andersen, S.T., 1965. Interglacialer og interstadialer i Danmarks kvartær. Med. Dan. Geol. Foren. 15, 486–506.
Bahain, J.-J., Falguères, C., Laurent, M., Dolo, J.-M., Shao, Q., Auguste, P., Tuffreau, A., 2015. ESR/U-series dating of faunal remains from the paleoanthropological site of Biache-Saint-Vaast (Pas-de-Calais, France). Quat. Geochronol. 30, 541–546.
Beerten, K., Heyvaert, V.M.A., Vandenberghe, D.A.G., Van Nieuland, J., Bogemans, F., 2017. Revising the Gent Formation: a new lithostratigraphy for Quaternary wind-dominated sand deposits in Belgium. Geol. Belg. 20, 95–102.
Behre, K.-E., 1989. Biostratigraphy of the last glacial period in Europe. Quat. Sci. Rev. 8, 25–44.
Benda, L., Ehlers, J., Hallik, R., 1993. Holstein-interglazial. Geol. Jahrbuch Reihe 138.
Birks, H.H., Birks, H.J.B., 2004. The rise and fall of forests. Science 305, 484–485.
Bogemans, F., 1983. Kwartairgeologische opnamen in het Bos van A te Zemst. Professional Paper. Geol. Survey Belgium 202.
Bogemans, F., 1988. Thematische kwartairgeologische voorstellingen als toepassingsmodellen in de economische ontwikkeling. PhD thesis. Vrije Universiteit Brussel.
Bogemans, F., 1993. Quaternary geological mapping on basis of sedimentary properties in the eastern branch of the Flemish Valley (Sheets Boom-Mechelen & Vilvoorde-Zemst). Toelichtende verhandelingen voor de geologische en mijnkaarten van België 35.
Bogemans, F., 1996. Toelichting bij de Quartairgeologische Kaart - kaartblad 23, Mechelen. Vlaamse overheid. dienst Natuurlijke Rijkdommen.
Bogemans, F., 2014. Sedimentologische beschrijving en interpretatie van Pleistocene afzettingen in ongeroerde boringen van de westelijke kustvlakte. Professional Paper. Geol. Survey Belgium 317.
Bogemans, F., Caspar, J.-P., 1984. Bois de A, site des artefacts. Bulletin de la Société belge de Géologie 93, 245–248.
Bogemans, F., Paepe, R., 1982. Preliminaire resultaten van de Kwartairkaartering in de Zennevallei ten noorden van Brussel. Professional Paper. Geol. Survey Belgium 190.
Bowen, D.Q., 1978. Quaternary Geology : a Stratigraphic Framework for Multidisciplinary Work. Pergamon press, Oxford.
Brandon, A., Sumbler, M.G., 1991. The Balderton Sand and Gravel: pre-Ipswichian cold stage fluvial deposits near Lincoln, England. J. Quat. Sci. 6, 117–138.
Bridgland, D., Howard, A., White, M., White, T., 2014. Quaternary of the Trent. Oxbow Books.
Buffel, P., Matthijs, J., 2009. Toelichtingen bij de Geologische Kaart van Belgie Vlaams Gewest Kaartblad 31-39 Brussel - Nijvel 1:50.000. Belgische Geologische Dienst en Vlaamse overheid, afdeling Land en Bodembescherming, Ondergrond, Natuurlijke Rijkdommen.
Buffel, P., Vandenberghe, N., Vackier, M., 2009. Toelichtingen bij de Geologische kaart van België Vlaams Gewest kaartblad 23 Mechelen 1:50.000. Belgische Geologische Dienst en Vlaamse overheid, afdeling Land en Bodembescherming, Ondergrond, Natuurlijke Rijkdommen.
Candy, I., Schreve, D., 2007. Land–sea correlation of Middle Pleistocene temperate sub-stages using high-precision uranium-series dating of tufa deposits from southern England. Quat. Sci. Rev. 26, 1223–1235.
Chytrý, M., Horsák, M., Danihelka, J., Ermakov, N., German, D.A., Hájek, M., Hájková, P., Kočí, M., Kubešová, S., Lustyk, P., Nekola, J.C., Pavelková Řičánková, V., Preislerová, Z., Resl, P., Valachovič, M., 2019. A modern analogue of the Pleistocene steppe-tundra ecosystem in southern Siberia. Boreas 48, 36–56.
Cleveringa, P., Meijer, T., van Leeuwen, R.J.W., de Wolf, H., Pouwer, R., Lissenberg, T., Burger, A.W., 2000. The Eemian stratotype locality at Amersfoort in the central Netherlands: a re-evaluation of old and new data. Neth. J. Geosci. 79, 197–216.
Cohen, K.M., Gibbard, P.L., 2019. Global chronostratigraphical correlation table for the last 2.7 million years, version 2019 QI-500. Quat. Int. 500, 20–31.
de Beaulieu, J.-L., Andrieu-Ponel, V., Reille, M., Grüger, E., Tzedakis, C., Svobodova, H., 2001. An attempt at correlation between the Velay pollen sequence and the Middle Pleistocene stratigraphy from central Europe. Quat. Sci. Rev. 20, 1593–1602.
De Clercq, M., Missiaen, T., Wallinga, J., Zurita Hurtado, O., Versendaal, A., Mathys, M., De Batist, M., 2018. A well-preserved Eemian incised-valley fill in the southern north sea basin, Belgian continental Shelf - Coastal plain: implications for northwest European landscape evolution. Earth Surf. Process. Landforms 43, 1913–1942.
de Jong, J., 1988. Climatic variability during the past three million years, as indicated by vegetational evolution in northwest Europe and with emphasis on data from The Netherlands. Philos. Trans. R. Soc. Lond. B Biol. Sci. 318, 603–617.
De Moor, G., 1963. Bijdrage tot de kennis van de fysische landschapsvorming in Binnen-Vlaanderen. Tijdschrift van de Belgische Vereniging voor Aardrijkskundige Studies 32, 329–433.
De Moor, G., Lootens, M., 1975. Afzettingen met Corbicula fluminalis in het Leiedal tussen Deinze en St.-Baafs-Vijve. Natuurwetenschappelijk Tijdschrift 57, 165–184.
De Moor, G., Heyse, I., De Groote, V., 1978. An outcrop of Eemian and early Weichselian deposits at Beernem (N.W. Belgium). Bull. Belg. Ver. Geol. 87, 27–36.
Decleer, K., 2007. Europees beschermde natuur in Vlaanderen en het Belgisch deel van de Noordzee : habitattypen, dier- en plantensoorten. Brussel : Instituut voor natuur- en bosonderzoek (INBO).
Desprat, S., Sánchez Goñi, M.F., Turon, J.-L., Duprat, J., Malaizé, B., Peypouquet, J.-P., 2006. Climatic variability of Marine Isotope Stage 7: direct land–sea–ice correlation from a multiproxy analysis of a north-western Iberian margin deep-sea core. Quat. Sci. Rev. 25, 1010–1026.
Diehl, M., Sirocko, F., 2007. A new holsteinian pollen record from the dry maar at Döttingen (Eifel). In: Sirocko, F., Claussen, M., Sánchez Goñi, M.F., Litt, T. (Eds.), Developments in Quaternary Sciences. Elsevier, pp. 397–416.
Erd, K., 1970. Pollen-analytical classification of the middle pleistocene in the German Democratic Republic. Palaeogeogr. Palaeoclimatol. Palaeoecol. 8, 129–145.
Erd, K., 1973. Pollenanalytische Gliederung des Pleistozäns der Deutschen Demokratischen Republik. Z. Geol. Wiss. 1, 1087–1103.
Erd, K., 1987. Die Uecker-Warmzeit von Röpersdorf bei Prenzlau als neuer Interglazialtyp im Saale-Komplex der DDR. Z. Geol. Wiss. 15, 297–313.
Erdős, L., Ambarlı, D., Anenkhonov, O.A., Bátori, Z., Cserhalmi, D., Kiss, M., Kröel-Dulay, G., Liu, H., Magnes, M., Molnár, Z., Naqinezhad, A., Semenishchenkov, Y.A., Tölgyesi, C., Török, P., Jiménez-Alfaro, B., 2018. The edge of two worlds: a new review and synthesis on Eurasian forest-steppes. Appl. Veg. Sci. 21, 345–362.
Erdtman, G., Berglund, B., Praglowski, J., 1961. An introduction to a Scandinavian pollen flora. Grana Palynol. 2, 3–86.
Fægri, K., Iversen, J., Waterbolk, H.T., 1964. Textbook of Pollen Analysis, 2nd rev. Munksgaard, Copenhagen.
Felde, V.A., Flantua, S.G.A., Jenks, C.R., Benito, B.M., De Beaulieu, J.L., Kunes, P., Magri, D., Nalepka, D., Risebrobakken, B., ter Braale, C.J.F., Allen, J.R.M.,

Granoszewski, W., Helmens, K.F., Huntley, B., Kondratiene, O., Kalnina, L., Kupryjanowicz, M., Malkiewicz, M., Milner, A.M., Nita, M., Noryskiewicz, B., Pidek, I.A., Reille, M., Salonen, J.S., Seiriene, V., Winter, H., Tzedakis, P.C., Birks, H.J.B., 2020. Compositional turnover and variation in Eemian pollen sequences in Europe. Veg. Hist. Archaeobotany 29, 101–109.
Follieri, M., Magri, D., Sadori, L., 1988. A 250 000-years pollen record from Valle di Castiglione (Roma). Pollen Spores 30, 329–356.
Follieri, M., Magri, D., Sadori, L., 1989. Pollen stratigraphical synthesis from Valle di Castiglione (roma). Quat. Int. 3–4, 81–84.
Germonpré, M., 1985. Some preliminary results on the upper pleistocene mammals of the Bos van A at Zemst (Brabant, Belgium). Lutra 28, 113–120.
Germonpré, M., 1986. An anomalous reindeer Rangifer tarandus (L., 1758) skull from the Lower Weichselian at the Bos van A, Zemst (Brabant, Belgium). Lutra 29, 320–324.
Germonpré, M., 1993. Taphonomy of pleistocene mammal assemblages of the Flemish valley, Belgium. Bulletin van het Koninklijk Belgisch Instituut voor Natuurwetenschappen, Aardwetenschappen 63, 271–309.
Germonpré, M., 2003. Mammoth taphonomy of two fluvial sites from the Flemish Valley, Belgium. Deinsea 9, 171–184.
Germonpré, M., Bogemans, F., Van Neer, W., Grün, R., 1993. The dating of two Pleistocene mammal assemblages of the Flemish Valley, Belgium. Contrib. Tert. Quat. Geol. 30, 147–153.
Gibbard, P.L., Lewin, J., 2002. Climate and related controls on interglacial fluvial sedimentation in lowland Britain. Sediment. Geol. 151, 187–210.
Goeury, C., Beaulieu, J.L.d., 1979. A propos de la concentration du pollen a′ l'aide de la liqueur de Thoulet dans les sédiments minéraux. Pollen Spores 21, 230–251.
Grimm, E.C., 1987. CONISS: a FORTRAN 77 program for stratigraphically constrained cluster analysis by the method of incremental sum of squares. Comput. Geosci. 13, 13–35.
Gulinck, M., Paepe, R., Vanhoorne, R., 1971. De Nieuwe Sluis van Zemst: Hoofdstuk V, Geologische waarnemingen en interpretaties. Excavator Mei 1–19.
Gullentops, F., 1954. Contributions à la chronologie du Pléistocène et des formes du relief en Belgique, vol. XVIII. Mémoires de l'institut Géologique de l'Université de Louvain, pp. 125–252.
Gullentops, F., Paulissen, E., Vandenberghe, J., 1981. Fossil periglacial phenomena in NE- Belgium. Biul. Peryglac. 28, 345–365.
Gullentops, F., Bogemans, F., De Moor, G., Paulissen, E., Pissart, A., 2001. Quaternary lithostratigraphic units (Belgium). Geol. Belg. 4, 153–164.
Guthrie, R.D., 1990. Frozen Fauna of the Mammoth Steppe : the Story of Blue Babe. University of Chicago press, Chicago (Ill.).
Guthrie, R.D., 2001. Origin and causes of the mammoth steppe: a story of cloud cover, woolly mammal tooth pits, buckles, and inside-out Beringia. Quat. Sci. Rev. 20, 549–574.
Halet, F., 1933. Sur la présence de couches à Corbicula fluminalis Müller aux environs de Saint-Denis-Westrem. Bull. Soc. Belge Geol. Paleontol. Hydrol. 43, 111–116.
Halet, F., Lejeune de Schiervel, C., 1905. Étude géologique avec coupe résultant des sondages effectués à travers la vallée de la Senne. Bull. Soc. Belge Geol. Paleontol. Hydrol. 19, 365–376.
Hallik, R., 1960. Die Vegetationsentwicklung der Holstein-Warmzeit in Nordwestdeutschland und die Altersstellung der Kieselgurlager der südlichen Lüneburger Heide. Z. Dtsch. Geol. Ges. 112, 326–333.
Havinga, A.J., 1967. Palynology and pollen preservation. Rev. Palaeobot. Palynol. 2, 81–98.
Herbosch, A., Debacker, T.N., 2018. A new geological map of the outcrop areas of the Brabant Massif (Belgium). Geol. Belg. 21, 41–58.
Hérisson, D., Brenet, M., Cliquet, D., Moncel, M.-H., Richter, J., Scott, B., Van Baelen, A., Di Modica, K., De Loecker, D., Ashton, N., Bourguignon, L., Delagnes, A., Faivre, J.-P., Folgado-Lopez, M., Locht, J.-L., Pope, M., Raynal, J.-P., Roebroeks, W., Santagata, C., Turq, A., Van Peer, P., 2016. The emergence of the Middle Palaeolithic in north-western Europe and its southern fringes. Quat. Int. 411, 233–283.
Heyse, I., Demoulin, A., 2018. The Flemish valley: response of the Scheldt drainage system to climatic and Glacio-Eustatic oscillations. In: Demoulin, A. (Ed.), Landscapes and Landforms of Belgium and Luxembourg. Springer, Cham, pp. 297–311.
Hoek, W.Z., 1997a. Atlas to palaeogeography of Lateglacial vegetations – maps of Lateglacial and early Holocene landscape and vegetation in The Netherlands, with an extensive review of available palynological data. Nederl. Geogr. Stud. 231.
Hoek, W.Z., 1997b. Palaeogeography of Lateglacial vegetations: aspects of Lateglacial and early Holocene vegetation, abiotic landscape, and climate in The Netherlands. Nederl. Geogr. Stud. 230.
Iversen, J., 1954. The late-glacial flora of Denmark and its relation to climate and soil. Danmarks Geologiske Undersøgelse II. Række 80, 87–119.
Kasse, C., 2002. Sandy aeolian deposits and environments and their relation to climate during the Last Glacial Maximum and Lateglacial in northwest and central Europe. Prog. Phys. Geogr. Earth Environ. 26, 507–532.
Kasse, C., van der Woude, J.D., Woolderink, H.A.G., Schokker, J., 2022. Eemian to Early Weichselian regional and local vegetation development and sedimentary and geomorphological controls, Amersfoort Basin, The Netherlands. Neth. J. Geosci. 101, e7.
Keen, D.H., 1990. Significance of the record provided by Pleistocene fluvial deposits and their included molluscan faunas for palaeoenvironmental reconstruction and stratigraphy: case studies from the English Midlands. Palaeogeogr. Palaeoclimatol. Palaeoecol. 80, 25–34.
Kemp, R.A., 1985. A consideration of the use of the terms 'paleosol' and 'rubification'. Quat. Newsl. 45, 6–11.
Kiden, P., 1991. The Lateglacial and Holocene evolution of the middle and lower river Scheldt, Belgium. In: Starkel, L., Gregory, K.J., Thornes, J.B. (Eds.), Fluvial Processes in the Temperate Zone during the Last 15,000 Years: Temperate Palaeohydrology, pp. 283–299.
Kleinmann, A., Müller, H., Lepper, J., Waas, D., 2011. Nachtigall: a continental sediment and pollen sequence of the Saalian Complex in NW-Germany and its relationship to the MIS-framework. Quat. Int. 241, 97–110.
Kolstrup, E., 1980. Climate and stratigraphy in northwestern Europe between 30,000 B.P. and 13,000 B.P., with special reference to The Netherlands. Meded. Rijks Geol. Dienst 32, 181–253.
Koutsodendris, A., Dakos, V., Fletcher, W.J., Knipping, M., Kotthoff, U., Milner, A.M., Müller, U.C., Kaboth-Bahr, S., Kern, O.A., Kolb, L., Vakhrameeva, P., Wulf, S., Christanis, K., Schmiedl, G., Pross, J., 2023a. Atmospheric CO2 forcing on Mediterranean biomes during the past 500 kyrs. Nat. Commun. 14, 1664.
Koutsodendris, A., Dakos, V., Fletcher, W.J., Knipping, M., Kotthoff, U., Milner, A.M., Müller, U.C., Kaboth-Bahr, S., Kern, O.A., Kolb, L., Vakhrameeva, P., Wulf, S., Christanis, K., Schmiedl, G., Pross, J., 2023b. Pollen Data from Tenaghi Philippon (Greece) Spanning the Past 500 Kyrs. PANGAEA.
Kuneš, P., Pelánková, B., Chytrý, M., Jankovská, V., Pokorný, P., Petr, L., 2008. Interpretation of the last-glacial vegetation of eastern-central Europe using modern analogues from southern Siberia. J. Biogeogr. 35, 2223–2236.
Leriche, M., 1934-1935. Les "sables chamois": un gîte fossilifère nouveau à la base des "sables chamois" du Petit-Brabant, vol. 58. Annales de la Société Géologique de Belgique, pp. B76–B82.
Lisiecki, L.E., Raymo, M.E., 2005. A Pliocene-Pleistocene stack of 57 globally distributed benthic δ18O records. Paleoceanography 20, PA1003.
Lister, A.M., 2022. Mammoth evolution in the late middle pleistocene: the Mammuthus trogontherii-primigenius transition in Europe. Quat. Sci. Rev. 294, 107693.
Lister, A.M., Brandon, A., 1991. A pre-Ipswichian cold stage mammalian fauna from the Balderton Sand and Gravel, Lincolnshire, England. J. Quat. Sci. 6, 139–157.
Lister, A.M., Sher, A.V., 2001. The origin and evolution of the woolly mammoth. Science 294, 1094–1097.
Litt, T., Turner, C., 1993. Arbeitsergebnisse der Subkommission für Europäische Quartärstratigraphie: die Saalesequenz in der Typusregion (Berichte der SEQS 10). Eiszeitalt. Ggw. 43, 125–128.
Louwye, S., Deckers, J., Verhaegen, J., Adriaens, R., Vandenberghe, N., 2020. A review of the lower and middle Miocene of northern Belgium. Geol. Belg. 23, 137–156.
Maglio, V.J., 1973. Origin and evolution of the Elephantidae. Trans. Am. Phil. Soc. 63, 1–149.
Makaske, B., 2001. Anastomosing rivers: a review of their classification, origin and sedimentary products. Earth Sci. Rev. 53, 149–196.
Masi, Alessia, Bertini, Adele, Combourieu-Nebout, Nathalie, Francke, Alexander, Kouli, Katerina, Joannin, Sébastien, Mercuri, Anna Maria, Peyron, Odile, Torri, Paola, Wagner, Bernd, Zanchetta, Giovanni, Sinopoli, Gaia, Donders, Timme H., 2016. Pollen-based paleoenvironmental and paleoclimatic change at Lake Ohrid (south-eastern Europe) during the past 500 ka. Biogeosciences 13 (5), 1423–1437. https://doi.org/10.5194/bg-13-1423-2016. PANGAEA.
McManus, J.F., Oppo, D.W., Cullen, J.L., 1999. A 0.5-million-year record of millennial-scale climate variability in the North atlantic. Science 283, 971–975.
Meijer, T., Preece, R.C., 2000. A review of the occurrence of Corbicula in the pleistocene of north-west Europe. Neth. J. Geosci. 79, 241–255.
Menke, B., 1968. Beiträge zur Biostratigraphie des Mittelpleistozäns in Norddeutschland. Meyniana 18, 35–42.
Mol, J., Vandenberghe, J., Kasse, C., 2000. River response to variations of periglacial climate in mid-latitude Europe. Geomorphology 33, 131–148.
Monnier, G.F., 2006. The Lower/Middle Paleolithic periodization in western Europe: an evaluation. Curr. Anthropol. 47, 709–744.
Moore, P.D., Webb, J.A., 1978. An Illustrated Guide to Pollen Analysis. John Wiley & Sons, Incorporated.
Mostaert, F., De Moor, G., 1984. Eemian deposits in the neighbourhood of Brugge: a palaeogeographical and sea-level reconstruction. Bull. Belg. Ver. Geol. 93, 279–286.
Mostaert, F., De Moor, G., 1989. Eemian and Holocene sedimentary sequences on the Belgian coast and their meaning for sea level reconstruction. North Sea. In: Henriet, J.P., De Moor, G. (Eds.), The Quaternary and Tertiary Geology of the Southern Bight, pp. 137–148.
Ninkovich, D., Shackleton, N.J., 1975. Distribution, stratigraphic position and age of ash layer "L". in the Panama Basin region. Earth and Planetary Science Letters 27, 20–34.
North American Commission on Stratigraphic Nomenclature, 2005. North American stratigraphic Code. AAPG (Am. Assoc. Pet. Geol.) Bull. 89, 1547–1591.
Okuda, M., Yasuda, Y., Setoguchi, T., 2001. Middle to late pleistocene vegetation history and climatic changes at Lake Kopais, Southeast Greece. Boreas 30, 73–82.
Paepe, R., 1972. Sedimentological parameters for a continuous climatic evolution throughout the Weichselian. Boreas 1, 173–183.
Paepe, R., Vanhoorne, R., 1967. The Stratigraphy and Palaeobotany of the Late Pleistocene in Belgium. Toelichtende Verhandelingen voor de Geologische kaart en Mijnkaart van België. Geol. Survey Belgium 8.
Past Interglacials Working Group of PAGES, 2016. Interglacials of the last 800,000

years. Rev. Geophys. 54, 162–219.
Penkman, K.E.H., Preece, R.C., Bridgland, D.R., Keen, D.H., Meijer, T., Parfitt, S.A., White, T.S., Collins, M.J., 2013. An aminostratigraphy for the British Quaternary based on Bithynia opercula. Quat. Sci. Rev. 61, 111–134.
Preusser, F., Drescher-Schneider, R., Fiebig, M., Schlüchter, C., 2005. Re-Interpretation of the Meikirch pollen record, Swiss alpine Foreland, and implications for middle pleistocene chronostratigraphy. J. Quat. Sci. 20, 607–620.
Railsback, L.B., Gibbard, P.L., Head, M.J., Voarintsoa, N.R.G., Toucanne, S., 2015. An optimized scheme of lettered marine isotope substages for the last 1.0 million years, and the climatostratigraphic nature of isotope stages and substages. Quat. Sci. Rev. 111, 94–106.
Reille, M., Andrieu, V., De Beaulieu, J.-L., Guenet, P., Goeury, C., 1998. A Long Pollen Record from Lac du Bouchet, Massif Central, France: for the Period ca. 325 to 100 ka BP (OIS 9c to OIS 5e). Quat. Sci. Rev. 17, 1107–1123.
Reille, M., Beaulieu, J.-L.D., Svobodova, H., Andrieu-Ponel, V., Goeury, C., 2000. Pollen analytical biostratigraphy of the last five climatic cycles from a long continental sequence from the Velay region (Massif Central, France). J. Quat. Sci. 15, 665–685.
Richter, J., 2011. When did the middle Paleolithic Begin? In: Conard, N.J., Richter, J. (Eds.), Neanderthal Lifeways, Subsistence and Technology: One Hundred Fifty Years of Neanderthal Study. Springer Netherlands, Dordrecht, pp. 7–14.
Rieke, H.H., Chilingarian, G.V., 1974. Chapter 3: Mechanics of compaction and compaction models. In: Rieke, H.H., Chilingarian, G.V. (Eds.), Developments in Sedimentology. Elsevier, pp. 87–122.
Roebroeks, W., 1988. From find scatters to Early Hominid behaviour: a study of Middle Palaeolithic riverside settlements at Maastricht-Belvédère (The Netherlands). Analecta Praehist. Leidensia 21.
Roucoux, K.H., Tzedakis, P.C., de Abreu, L., Shackleton, N.J., 2006. Climate and vegetation changes 180,000 to 345,000 years ago recorded in a deep-sea core off Portugal. Earth Planet Sci. Lett. 249, 307–325.
Roucoux, K.H., Tzedakis, P.C., Frogley, M.R., Lawson, I.T., Preece, R.C., 2008. Vegetation history of the marine isotope stage 7 interglacial complex at Ioannina, NW Greece. Quat. Sci. Rev. 27, 1378–1395.
Ruddiman, W.F., Sancetta, C.D., McIntryre, A., Manley, G., Dreimanis, A., Lamb, H.H., Mitchell, G.F., West, R.G., 1977. Glacial/Interglacial response rate of subpolar North Atlantic waters to climatic change: the record in oceanic sediments. Philos. Trans. R. Soc. Lond. B Biol. Sci. 280, 119–142.
Rutot, A.L., 1910. Sur la découverte de Corbicula fluminalis à Hofstade. Académie royale de Belgique. Bulletin de la Classe des sciences 164–169.
Rutot, A.L., Van den Broeck, E., 1892. Résultats géologiques des sondages exécutés entre Bruxelles et le Rupel par les soins de la Commission des Installations Maritimes de Bruxelles. Bull. Soc. Belge Geol. Paleontol. Hydrol. 6, 53–67.
Sadori, L., Koutsodendris, A., Panagiotopoulos, K., Masi, A., Bertini, A., Combourieu-Nebout, N., Francke, A., Kouli, K., Joannin, S., Mercuri, A.M., Peyron, O., Torri, P., Wagner, B., Zanchetta, G., Sinopoli, G., Donders, T.H., 2016. Pollen-based paleoenvironmental and paleoclimatic change at Lake Ohrid (south-eastern Europe) during the past 500 ka. Biogeosciences 13, 1423–1437.
Sadori, L., Koutsodendris, A., Panagiotopoulos, K., Masi, A., Bertini, A., Combourieu-Nebout, N., Francke, A., Kouli, K., Kousis, I., Joannin, S., Mercuri, A.M., Peyron, O., Torri, P., Wagner, B., Zanchetta, G., Sinopoli, G., Donders, T.H., 2018. Pollen data of the last 500 ka BP at Lake Ohrid (south-eastern Europe), supplement to: Sadori, Laura; Koutsodendris. Andreas; Panagiotopoulos, Konstantinos.
Sánchez Goñi, M.F., Loutre, M.F., Crucifix, M., Peyron, O., Santos, L., Duprat, J., Malaizé, B., Turon, J.L., Peypouquet, J.P., 2005. Increasing vegetation and climate gradient in Western Europe over the Last Glacial Inception (122–110 ka): data-model comparison. Earth Planet Sci. Lett. 231, 111–130.
Schirmer, W., 2010. Interglacial complex and solcomplex. Open Geosci. 2, 32–40.
Schokker, J., Cleveringa, P., Murray, A.S., Wallinga, J., Westerhoff, W.E., 2005. An OSL dated middle and late quaternary sedimentary record in the roer valley Graben (southeastern Netherlands). Quat. Sci. Rev. 24, 2243–2264.
Schreve, D., 2019. All is flux: the predictive power of fluctuating Quaternary mammalian faunal-climate scenarios. Philos. Trans. R. Soc. Lond. Ser. B Biol. Sci. 374, 20190213.
Scott, K., Buckingham, C., 2021. Mammoths and Neanderthals in the Thames Valley: Excavations at Stanton Harcourt, Oxfordshire. Archaeopress, Oxford.
Suggate, R.P., 1965. The definition of "interglacial". J. Geol. 73, 619–626.
Sutcliffe, A.J., Kowalski, K., 1976. Pleistocene rodents of the British isles. Bull. Br. Museum (Nat. Hist.) 27, 31–147.
Tavernier, R., 1954. Le quaternaire. In: Fourmarier, P. (Ed.), Prodrome d'une description géologique de la Belgique. Vaillant-Carmanne, Liège, pp. 555–589.
Tucci, M., Krahn, K.J., Richter, D., van Kolfschoten, T., Álvarez, B.R., Verheijen, I., Serangeli, J., Lehmann, J., Degering, D., Schwalb, A., Urban, B., 2021. Evidence for the age and timing of environmental change associated with a Lower Palaeolithic site within the Middle Pleistocene Reinsdorf sequence of the Schöningen coal mine. Germany Palaeogeogr. Palaeoclimatol. Palaeoecol. 569.
Tuffreau, A., Sommé, J., 1988. Le gisement paléolithique moyen de Biache-Saint-Vaast (Pas-de-Calais). Mémoires de la Société Préhistorique Française 21.
Turner, C., 1989. Type sections and Quaternary deposits. In: Rose, J., Schlüchter, C. (Eds.), Quaternary Type Sections: Imagination or Reality?, pp. 41–44.
Turner, C., 1998. Volcanic Maars, long quaternary sequences and the work of the INQUA Subcommission on European quaternary stratigraphy. Quat. Int. 47–48, 41–49.
Turner, C., 2000. The Eemian interglacial in the North European plain and adjacent areas. Geol Mijnbouw-N J G 79, 217–231.
Turner, C., West, R.G., 1968. The subdivision and zonation of interglacial periods. Eiszeitalt. Ggw. 19, 93–101.
Turq, A., 2000. Le Moustérien Typique. Paléo. Revue d'Archéologie Préhistorique, supplément, pp. 274–291.
Tzedakis, P.C., Andrieu, V., de Beaulieu, J.L., Crowhurst, S., Follieri, M., Hooghiemstra, H., Magri, D., Reille, M., Sadori, L., Shackleton, N.J., Wijmstra, T.A., 1997. Comparison of terrestrial and marine records of changing climate of the last 500,000 years. Earth Planet Sci. Lett. 150, 171–176.
Tzedakis, P.C., Roucoux, K.H., de Abreu, L., Shackleton, N.J., 2004. The duration of forest stages in southern Europe and interglacial climate variability. Science 306, 2231–2235.
Urban, B., 1995. Palynological evidence of younger middle pleistocene interglacials (holsteinian, reinsdorf and schöningen) in the schöningen open cast lignite mine (eastern lower Saxony, Germany). Meded. Rijks Geol. Dienst 52, 175–185.
Urban, B., 2007. Interglacial pollen records from schöningen, North Germany. In: Sirocko, F., Claussen, M., Sánchez Goñi, M.F., Litt, T. (Eds.), Developments in Quaternary Sciences. Elsevier, pp. 417–444.
Urban, B., Lenhard, R., Mania, D., Albrecht, B., 1991. Mittelpleistozän im Tagebau Schöningen, Ldkr. Helmstedt. Z. Dtsch. Geol. Ges. 142, 351–372.
Van der Sluys, J., 1996. Geologisch Onderzoek langs de hoge-snelheidslijn tussen Brussel en Leuven. Professional Paper, Geological Survey of Belgium 282.
van Huissteden, J., Gibbard, P.L., Briant, R.M., 2001. Periglacial fluvial systems in northwest Europe during marine isotope stages 4 and 3. Quat. Int. 79, 75–88.
Van Kolfschoten, T., Roebroeks, W., 1985. Maastricht-Belvédère: stratigraphy, palaeoenvironment and archaeology of the Middle and Late Pleistocene deposits. Meded. Rijks Geol. Dienst 39, 1–121.
Van Peer, P., Smith, R., 1990. Zemst "Bos van Aa": Un site du Paléolithique moyen de la partie orientale de la vallée Flamande. Helinium XXX, 157–171.
Vandenberghe, J., Woo, M.-k., 2002. Modern and ancient periglacial river types. Prog. Phys. Geogr. Earth Environ. 26, 479–506.
Vandenberghe, J., Roebroeks, W., Van Kolfschoten, T., 1993. Maastricht-Belvédère: stratigraphy, palaeoenvironment and archaeology of the Middle and Late Pleistocene deposits; Part II. Meded. Rijks Geol. Dienst 47, 1–91.
Verbruggen, C., 1982. Late Middle-Pleistocene Pollensequences from Flanders (Belgium) [abstract], XI INQUA Congress. International Union for Quaternary Research, Moscow.
Verbruggen, C., 1999. Quaternary palaeobotanical evolution of northern Belgium. Geol. Belg. 2, 99–110.
Wansa, S., 2019. Zur Geologie des Ummendorfer Kessels im oberen Allertal: Forschungsbohrung Ummendorf 1/2012. Mitteilungen zu Geologie und Bergwesen von Sachsen-Anhalt 20.
Wijmstra, T.A., Smit, A., 1976. Palynology of the middle part (30-78 metres) of the 120 m deep section in Northern Greece (Macedonia). Acta Bot. Neerl. 25, 297–312.
Zagwijn, W.H., 1961. Vegetation, climate and radiocarbon datings in the late pleistocene of The Netherlands. Part I: Eemian and early Weichselian. Meded. Rijks Geol. Dienst 14, 15–45.
Zagwijn, W.H., 1973. Pollenanalytic studies of holsteinian and Saalian beds in the northern Netherlands. Meded. Rijks Geol. Dienst 24, 139–156.
Zagwijn, W.H., 1996. An analysis of Eemian climate in western and central Europe. Quat. Sci. Rev. 15, 451–469.
Zagwijn, W., Paepe, R., 1968. Die Stratigraphie der weichselzeitlichen Ablagerungen der Niederlande und Belgiens. Eiszeitalt. Ggw. 19, 129–146.